

Color Image Inpainting via Robust Pure Quaternion Matrix Completion: Error Bound and Weighted Loss

Junren Chen*

Michael K. Ng[†]

Abstract

In this paper, we study color image inpainting as a pure quaternion matrix completion problem. In the literature, the theoretical guarantee for quaternion matrix completion is not well-established. Our main aim is to propose a new minimization problem with an objective combining nuclear norm and a quadratic loss weighted among three channels. To fill the theoretical vacancy, we obtain the error bound in both clean and corrupted regimes, which relies on some new results of quaternion matrices. A general Gaussian noise is considered in robust completion where all observations are corrupted. Motivated by the error bound, we propose to handle unbalanced or correlated noise via a cross-channel weight in the quadratic loss, with the main purpose of rebalancing noise level, or removing noise correlation. Extensive experimental results on synthetic and color image data are presented to confirm and demonstrate our theoretical findings.

1 Introduction

Compared with gray images, color images contain three highly-correlated channels, i.e., R (red), G (green) and B (blue). A direct method in color image processing is the monochromatic model, which applies the well-developed gray image processing techniques to each channel separately, but usually results in performance degradation since it fails to capture the correlations among three channels [10,13,22,43,49]. In addition, the concatenation model [48,49] deals with the gray image obtained by unfolding and concatenating three channels, but it still cannot make full use of the couplings.

As an expansion of complex number, quaternion numbers contain one real part, three imaginary parts, they form the non-commutative field \mathbb{Q} . We can completely capture the couplings among three channels by encoding RGB values into three imaginary parts of quaternion, then process color images as a whole under the non-trivial algebra structure of \mathbb{Q} . Therefore, \mathbb{Q} has been noted to be a suitable platform for color image processing.

The idea of using quaternion to represent and process color image can be traced back to relatively old work such as [36, 37, 39]. After these initial applications, many classical tools in \mathbb{R} or \mathbb{C} were extended to \mathbb{Q} , to name a few, singular value decomposition [54] and its applications [8, 26], Fourier transform [16, 39], PCA [43], wavelet transform [2], moments analysis [10, 11]. Moreover, some color image processing techniques based on quaternion were

*Department of Mathematics, The University of Hong Kong. E-mail: chenjr58@connect.hku.hk

[†]Department of Mathematics, The University of Hong Kong. E-mail: mng@maths.hku.hk

established, including denoising [9,13,19,22,53], inpainting [21,24,28,31], segmentation [40,42], watermarking [1], super-resolution [52], neural network [35,55], and so forth.

Thanks to the non-local self-similarity [14], it is reasonable to assume natural images are (approximately) low-rank, thus, color image inpainting can be cast as a low-rank quaternion matrix completion problem. Since a rank minimization problem is generally NP-hard [20], we resort to rank surrogate that is computationally feasible. It has been proved that the nuclear norm is the tightest convex surrogate of the rank of quaternion matrices [24], and undoubtedly nuclear norm is most frequently used [21,23,24,30,31]. In pursuit of more precise approximation to rank, recent papers proposed to use non-convex surrogates that penalize large singular value less [13,50,51,53], or some regularizers based on matrix factorization [28, 29], which avoids computing SVD of a large quaternion matrix but requires a prior estimation of the rank. Using quaternion to inpaint color image leads to exciting inpainting quality and impressive experimental performance, we notice that more recent papers even began to study recovering color videos via quaternion tensor [23,30].

While existing work focused on algorithms, novel regularizers and experimental results, theoretical guarantees on reconstruction error are extremely rare. To our best knowledge, [24] is the only paper that provided exact recovery guarantee for low-rank quaternion matrix satisfying the incoherence condition [6,7,38]. However, it is impractical to assume natural images satisfy incoherence condition, which is stringent, unstable, and hard to verify. Without theoretical support on the recovery error, even the algorithms can perfectly find the global minimum point, the obtained quaternion matrix (i.e., reconstructed image) is not guaranteed to well approximate the underlying matrix (i.e., original image), hence quaternion-based inpainting method can only be an empirical success.

We fill the theoretical vacancy in this paper. We study the most classical quaternion inpainting method that uses nuclear norm as rank surrogate, and obtain the reconstructed error bound. Our results are established under much weaker conditions compared with [24]: the stringent incoherence condition is removed, and the the original image is only assumed to be approximately low-rank, which is a relaxation of exact low-rankness. In regard to the robustness, we handle i.i.d. additive Gaussian noises distributed over the whole image, while [24] requires the noise to be sufficiently sparse. As a refinement, we restrict to pure quaternion matrix [41] with non-negative imaginary parts, for the RGB values of a pixel are non-negative. In comparison, most existing papers (e.g., [24,29,30]) neglect the "zero real part" constraint and choose to drop the real part of the reconstructed quaternion matrix, then the obtained pure quaternion matrix is not the best approximation, and more severely, it may not be low-rank, see Remark 1. As to the technical proof, our work is inspired by [25], and can be viewed as an extension to quaternion and approximate low-rankness (note that the result in [25] requires exact low-rankness).

Moreover, we introduce a corss-channel weight in the loss function. When the noises in three channels have extremely different scales or are highly-correlated, we develop a noise correction strategy to rebalance the noise level, or remove the noise correlations. In brief, our main contributions can be summarized as follows:

- We obtain the error bound of quaternion-based color image inpainting method that uses nuclear norm as rank surrogate. The error bound fills theoretical vacancy and manages to support existing literature. The established framework also encompasses the completion of a general quaternion matrix.

- We consider general Gaussian noise in the corrupted model. To better achieve robustness under unbalanced or correlated noise, we propose a noise correction strategy that relies on a cross-channel weight in the loss function.

Besides, it is worthy to mention that the technical proof of our main results, some lemmas on norm or concentration of quaternion matrix may be of independent interest.

The paper is organized in this way: In Section 2 we provide preliminaries of quaternion and state the notations; In Section 3 we present our main results, including the reconstructed error bound under both clean and corrupted situations, and a noise correction strategy; In Section 4 we use alternating direction method of multipliers (ADMM) to solve the proposed optimization problem, and report experimental results on both synthetic and color image data to demonstrate and verify our theoretical findings; In Section 5 some concluding remarks are given. For clarity all proofs are collected in Appendix A, B.

2 Preliminaries and Notations

In principle, we use boldface lowercase letters (e.g., \mathbf{q} , $\boldsymbol{\epsilon}$) to denote quaternion numbers, while boldface capital letters (e.g., \mathbf{X} , $\boldsymbol{\Theta}$) represent matrices that can be real, complex or quaternionic. One exception is that we use Y_1, \dots, Y_n to denote the n observed values, which are quaternion basically.

Let \mathbb{Q} be the set of quaternion, and $\mathbf{q} = q_0 \mathbf{1} + q_1 \mathbf{i} + q_2 \mathbf{j} + q_3 \mathbf{k}$ be a quaternion with $q_0 \in \mathbb{R}$ as the real part (component), $q_1, q_2, q_3 \in \mathbb{R}$ as three imaginary parts (components). The addition and subtraction of two quaternion numbers are operated component-wisely. By the regulation

$$\begin{aligned} \mathbf{i}^2 = \mathbf{j}^2 = \mathbf{k}^2 = -1; \quad \mathbf{i}\mathbf{j} = -\mathbf{j}\mathbf{i} = \mathbf{k}; \\ \mathbf{j}\mathbf{k} = -\mathbf{k}\mathbf{j} = \mathbf{i}; \quad \mathbf{k}\mathbf{i} = -\mathbf{i}\mathbf{k} = \mathbf{j} \end{aligned}$$

and distributive law, the multiplication can be defined naturally. Note that the multiplication is non-commutative. We use $[\cdot]_{\mathbf{1}}, [\cdot]_{\mathbf{i}}, [\cdot]_{\mathbf{j}}, [\cdot]_{\mathbf{k}}$ to extract the corresponding component of a quaternion number, vector or matrix, for example, $[\mathbf{q}]_{\mathbf{1}} = q_0$, $[\mathbf{q}]_{\mathbf{j}} = q_j$. Sometimes we also use the more standard notation $\text{Re}(\cdot)$ to extract the real part, while $\text{Im}(\mathbf{q}) = q_1 \mathbf{i} + q_2 \mathbf{j} + q_3 \mathbf{k}$ is the whole imaginary part. The conjugate of \mathbf{q} is given by $\overline{\mathbf{q}} = q_0 \mathbf{1} - q_1 \mathbf{i} - q_2 \mathbf{j} - q_3 \mathbf{k}$, and we have

$$\mathbf{q}\overline{\mathbf{q}} = q_0^2 + q_1^2 + q_2^2 + q_3^2 = |\mathbf{q}|^2,$$

where $|\mathbf{q}|$ is called the absolute value or magnitude of \mathbf{q} . The inverse of nonzero \mathbf{q} is $\mathbf{q}^{-1} = \overline{\mathbf{q}}/|\mathbf{q}|^2$, by which the division is defined immediately.

Consider a quaternion matrix $\mathbf{A} = [\mathbf{a}_{ij}], \mathbf{B} = [\mathbf{b}_{ij}] \in \mathbb{Q}^{M \times N}$, we let $\overline{\mathbf{A}} = [\overline{\mathbf{a}_{ij}}]$ be the conjugate, $\mathbf{A}^T = [\mathbf{a}_{ji}] \in \mathbb{Q}^{N \times M}$ be the transpose, and $\mathbf{A}^* = \overline{\mathbf{A}}^T = [\overline{\mathbf{a}_{ji}}] \in \mathbb{Q}^{N \times M}$ be the conjugate transpose. We define the standard inner product in $\mathbb{Q}^{M \times N}$ by

$$\langle \mathbf{A}, \mathbf{B} \rangle = \text{Tr}(\mathbf{A}^* \mathbf{B}) = \sum_{i=1}^M \sum_{j=1}^N \overline{\mathbf{a}_{ij}} \mathbf{b}_{ij}.$$

The rank of \mathbf{A} is defined to be the maximum number of right linearly independent columns vectors of \mathbf{A} . If $\mathbf{A} \in \mathbb{Q}^{N \times N}$ and $\text{rank}(\mathbf{A}) = N$, then \mathbf{A} is invertible, and the inverse is denoted

by \mathbf{A}^{-1} satisfying $\mathbf{A}\mathbf{A}^{-1} = \mathbf{A}^{-1}\mathbf{A} = \mathbf{I}_N$. \mathbf{A} is unitary if \mathbf{A} is invertible and $\mathbf{A}^{-1} = \mathbf{A}^*$, \mathbf{A} is Hermitian if $\mathbf{A}^* = \mathbf{A}$.

Quaternion singular value decomposition (QSVD) was introduced in [54]. Given $\mathbf{A} \in \mathbb{Q}^{M \times N}$, there exist unitary matrices $\mathbf{U} \in \mathbb{Q}^{M \times M}$, $\mathbf{V} \in \mathbb{Q}^{N \times N}$, and diagonal matrix $\Sigma = \text{diag}(\sigma_1(\mathbf{A}), \sigma_2(\mathbf{A}), \dots, \sigma_{\min\{M,N\}}(\mathbf{A})) \in \mathbb{Q}^{M \times N}$ such that

$$\mathbf{A} = \mathbf{U}\Sigma\mathbf{V}^*, \quad (2.1)$$

where non-negative numbers $\sigma_1(\mathbf{A}) \geq \sigma_2(\mathbf{A}) \geq \dots \geq \sigma_{\min\{M,N\}}(\mathbf{A})$ are the singular values of \mathbf{A} . Parallel to complex matrices, $\text{rank}(\mathbf{A})$ equals the number of positive singular values of \mathbf{A} . We work with different matrix norms. The nuclear norm is defined to be the sum of singular values, i.e., $\|\mathbf{A}\|_{\text{nu}} = \sum_i \sigma_i(\mathbf{A})$. Besides, we define the Frobenius norm, operator norm, $\|\cdot\|_{2,\infty}$ and max norm as ($[k] = \{1, \dots, k\}$)

$$\begin{aligned} \|\mathbf{A}\|_{\text{F}} &= \left[\sum_{i \in [M]} \sum_{j \in [N]} |\mathbf{a}_{ij}|^2 \right]^{1/2}, \quad \|\mathbf{A}\|_{\text{op}} = \sup_{\mathbf{x} \in \mathbb{Q}^N \setminus \{0\}} \frac{\|\mathbf{A}\mathbf{x}\|_2}{\|\mathbf{x}\|_2} \\ \|\mathbf{A}\|_{2,\infty} &= \max_{i \in [M]} \left[\sum_{j \in [N]} |\mathbf{a}_{ij}|^2 \right]^{1/2}, \quad \|\mathbf{A}\|_{\infty} = \max_{(i,j) \in [M] \times [N]} |\mathbf{a}_{ij}|, \end{aligned}$$

where $\|\cdot\|_2$ is the ℓ_2 norm of a vector. It is interesting to note that

$$\|\mathbf{A}\|_{\text{F}} = \left[\sum_i \sigma_i(\mathbf{A})^2 \right]^{1/2}, \quad \|\mathbf{A}\|_{\text{op}} = \sigma_1(\mathbf{A}).$$

Another powerful tool to study quaternion matrices is the so-called complex adjoint matrix. Note that $\mathbf{A} \in \mathbb{Q}^{M \times N}$ can be uniquely written as $\mathbf{A}^{(1)} + \mathbf{A}^{(2)}\mathbf{j}$ where $\mathbf{A}^{(1)}, \mathbf{A}^{(2)} \in \mathbb{C}^{M \times N}$, then the complex adjoint matrix is given by

$$[\mathbf{A}]_{\mathbb{C}} = \begin{bmatrix} \mathbf{A}^{(1)} & \mathbf{A}^{(2)} \\ -\mathbf{A}^{(2)} & \mathbf{A}^{(1)} \end{bmatrix} \in \mathbb{C}^{2M \times 2N}, \quad (2.2)$$

which preserves not only addition, subtraction, but also multiplication, conjugate transpose, inverse (Theorem 4.2, [54]), e.g., $[\mathbf{A}^*]_{\mathbb{C}} = [\mathbf{A}]_{\mathbb{C}}^*$, $[\mathbf{AC}]_{\mathbb{C}} = [\mathbf{A}]_{\mathbb{C}}[\mathbf{C}]_{\mathbb{C}}$ where $\mathbf{C} \in \mathbb{Q}^{N \times P}$. If necessary, \mathbf{A} can be further reduced to a $4M \times 4N$ real matrix, see for example [41].

A quaternion with zero real part is called pure quaternion, and the set of pure quaternion numbers is denoted by \mathbb{Q}_{pure} . Tailored to pixels of color image we consider pure quaternion with non-negative imaginary parts, which is called "pixel quaternion" and collected in the set

$$\mathbb{Q}_{\text{pix}} = \{q_1 \mathbf{i} + q_2 \mathbf{j} + q_3 \mathbf{k} : q_1, q_2, q_3 \in \mathbb{R}_{\geq 0}\}.$$

We mainly deal with pixel quaternion in this paper.

As a generalization of the quadratic loss, we consider a weighted loss where the weight $\mathbf{W} \in \mathbb{R}^{3 \times 3}$ is a positive definite matrix, and $\sqrt{\mathbf{W}}$ stands for its square root. A pure quaternion $\mathbf{q} = q_1 \mathbf{i} + q_2 \mathbf{j} + q_3 \mathbf{k}$ is identified as 3-dimensional real vector $[q_1, q_2, q_3]^T \in \mathbb{R}^3$ when operating with $\mathbf{W} = [w_{ij}]$, for example,

$$\begin{cases} \mathbf{W}\mathbf{q} &= (\sum_{i=1}^3 w_{1i}q_i) \mathbf{i} + (\sum_{i=1}^3 w_{2i}q_i) \mathbf{j} + (\sum_{i=1}^3 w_{3i}q_i) \mathbf{k} \\ \mathbf{q}^T \mathbf{W} \mathbf{q} &= \sum_{i=1}^3 \sum_{j=1}^3 q_i w_{ij} q_j \end{cases}.$$

Moreover, we allow \mathbf{W} to element-wisely operate on $\mathbf{A} = [\mathbf{a}_{ij}] \in \mathbb{Q}^{M \times N}$, i.e., $\mathbf{W}\mathbf{A} = [\mathbf{W}\mathbf{a}_{ij}] \in \mathbb{Q}^{M \times N}$. Since \mathbf{W} is not restricted to be diagonal matrix, it introduces more flexibility in dealing with RGB correlations, see the noise correction strategy proposed in this work. For convenience we define the weighted magnitude of $\mathbf{q} \in \mathbb{Q}_{\text{pure}}$ to be $|\mathbf{q}|_w = \sqrt{\mathbf{q}^T \mathbf{W} \mathbf{q}}$, and the weighted Frobenius norm, weighted max norm of $\mathbf{A} \in \mathbb{Q}_{\text{pure}}^{M \times N}$ are given by

$$\|\mathbf{A}\|_{w,F} = \left[\sum_{i \in [M]} \sum_{j \in [N]} |\mathbf{a}_{ij}|_w^2 \right]^{1/2}; \quad \|\mathbf{A}\|_{w,\infty} = \max_{i,j} |\mathbf{a}_{ij}|_w.$$

Evidently, we have $|\mathbf{q}|_w = |\sqrt{\mathbf{W}}\mathbf{q}|$, $\|\mathbf{A}\|_{w,F} = \|\sqrt{\mathbf{W}}\mathbf{A}\|_F$, $\|\mathbf{A}\|_{w,\infty} = \|\sqrt{\mathbf{W}}\mathbf{A}\|_\infty$.

The proof of our main results relies on some statistical methods. We use $\mathbb{E}(\cdot)$ and $\mathbb{P}(\cdot)$ to denote the expectation and the probability, respectively. Besides, if there exists an absolute constant C , such that $B_1 \leq CB_2$, then we write $B_1 \lesssim B_2$, we also use $B_1 \gtrsim B_2$ to represent the converse inequality. We consider random Gaussian noise $\boldsymbol{\epsilon} \in \mathbb{Q}_{\text{pure}}$ and assume that $([\boldsymbol{\epsilon}]_i, [\boldsymbol{\epsilon}]_j, [\boldsymbol{\epsilon}]_k)^T \sim \mathcal{N}(0, \boldsymbol{\Sigma}_c)$, where $\boldsymbol{\Sigma}_c \in \mathbb{R}^{3 \times 3}$ is the positive definite covariance matrix.

To prove our main results we establish some technical tools for quaternion matrices, the proof can be found in Appendix A. Lemma 1, Lemma 2 extend two well-known inequalities for complex matrices to quaternion matrices.

Lemma 1. *Assume $\mathbf{A} \in \mathbb{Q}^{M \times N}$, then $\|\mathbf{A}\|_{\text{nu}} \leq \sqrt{\text{rank}(\mathbf{A})} \|\mathbf{A}\|_F$.*

Lemma 2. *Assume $\mathbf{A}, \mathbf{B} \in \mathbb{Q}^{M \times N}$, then $|\langle \mathbf{A}, \mathbf{B} \rangle| \leq \|\mathbf{A}\|_{\text{op}} \|\mathbf{B}\|_{\text{nu}}$.*

Lemma 3 shows the relationship between nuclear norm of quaternion matrix and its four components, while Corollary 1 is given in a generalized form.

Lemma 3. *Assume $\mathbf{A} = \mathbf{A}_0 + \mathbf{A}_1 \mathbf{i} + \mathbf{A}_2 \mathbf{j} + \mathbf{A}_3 \mathbf{k} \in \mathbb{Q}^{M \times N}$ where $\mathbf{A}_0, \mathbf{A}_1, \mathbf{A}_2, \mathbf{A}_3 \in \mathbb{R}^{M \times N}$, then we have $\|\mathbf{A}\|_{\text{nu}} \geq \|\mathbf{A}_0 + \mathbf{A}_1 \mathbf{i}\|_{\text{nu}} \geq \|\mathbf{A}_0\|_{\text{nu}}$.*

Corollary 1. *Under the setting of Lemma 3, we consider $\boldsymbol{\nu} = (\nu_0, \nu_1, \nu_2, \nu_3)^T \in \mathbb{R}^4$, $\|\boldsymbol{\nu}\|_2 = 1$. Then we have $\|\mathbf{A}\|_{\text{nu}} \geq \|\nu_0 \mathbf{A}_0 + \nu_1 \mathbf{A}_1 + \nu_2 \mathbf{A}_2 + \nu_3 \mathbf{A}_3\|_{\text{nu}}$.*

Remark 1. *Lemma 3 states that $\|\mathbf{A}\|_{\text{nu}} \geq \max\{\|\mathbf{A}_0 + \mathbf{A}_1 \mathbf{i}\|_{\text{nu}}, \|\mathbf{A}_2 \mathbf{j} + \mathbf{A}_3 \mathbf{k}\|_{\text{nu}}\}$, which cannot be further improved to $\|\mathbf{A}\|_{\text{nu}} \geq \|\mathbf{A}_1 \mathbf{i} + \mathbf{A}_2 \mathbf{j} + \mathbf{A}_3 \mathbf{k}\|_{\text{nu}}$. We consider*

$$\mathbf{A} = \begin{bmatrix} 1 + 3\mathbf{i} & \mathbf{k} - 3\mathbf{j} \\ 1 + 3\mathbf{j} & \mathbf{k} + 3\mathbf{i} \end{bmatrix},$$

by removing the real component we obtain

$$\mathbf{A}_p = \begin{bmatrix} 3\mathbf{i} & \mathbf{k} - 3\mathbf{j} \\ 3\mathbf{j} & \mathbf{k} + 3\mathbf{i} \end{bmatrix}.$$

It is not hard to verify $\|\mathbf{A}_p\|_{\text{nu}} > \|\mathbf{A}\|_{\text{nu}}$. Moreover, $\text{rank}(\mathbf{A}) = 1 < \text{rank}(\mathbf{A}_p) = 2$, showing that removing the real part of a low-rank quaternion matrix may destroy the low-rankness. Therefore, restriction to pure quaternion is important when dealing with color image inpainting.

Finally we provide the moment constraint version Bernstein inequality for quaternion matrices, which is an extension of Theorem 6.2 in [44]. Although our main result (Theorem 2) is presented under multi-variate Gaussian noise, it directly extends to more general sub-exponential noise that satisfies the moment constraint (2.3).

Lemma 4. Let $\mathbf{S}_1, \mathbf{S}_2, \dots, \mathbf{S}_n \in \mathbb{Q}^{M \times M}$ be independent, Hermitian random quaternion matrices with zero mean, assume that for integer $p \geq 2$, there exist $R, \sigma > 0$ such that

$$\|\mathbb{E} \mathbf{S}_k^p\|_{\text{op}} \leq \frac{1}{2} p! R^{p-2} \sigma^2. \quad (2.3)$$

Then for any $t > 0$ we have

$$\mathbb{P} \left[\left\| \frac{1}{n} \sum_{k=1}^n \mathbf{S}_k \right\|_{\text{op}} \geq t \right] \leq 4M \exp \left(-\frac{nt^2}{2(\sigma^2 + Rt)} \right). \quad (2.4)$$

3 Main results

Let $\tilde{\Theta} = [\tilde{\theta}_{ij}] \in \mathbb{Q}_{\text{pix}}^{d_1 \times d_2}$ be the desired original color image, assume that we make n observations in total ($n \leq d_1 d_2$), and $\mathbf{X}_1, \dots, \mathbf{X}_n$ are i.i.d. uniformly distributed over $\{e_i e_j^T : i \in [d_1], j \in [d_2]\}$, or equivalently, assume $\mathbf{X}_k = e_{k(i)} e_{k(j)}^T$ where $(k(i), k(j)) \sim \text{unif}([d_1] \times [d_2])$. Note that e_i is the vector whose i -th entry is 1 and other entries are 0, and $e_i \in \mathbb{R}^{d_1}$, $e_j \in \mathbb{R}^{d_2}$ in $e_i e_j^T \in \mathbb{R}^{d_1 \times d_2}$, but we omit the dimension for simplicity. By using $\langle e_i e_j^T, \tilde{\Theta} \rangle = \tilde{\theta}_{ij}$ to represent observing the (i,j) -pixel, the clean model where the precise value of the entry is available can be formulated as

$$Y_k = \langle \mathbf{X}_k, \tilde{\Theta} \rangle. \quad (3.1)$$

We also consider the robust completion problem where observations are corrupted by pure quaternion noise, i.e.,

$$Y_k = \langle \mathbf{X}_k, \tilde{\Theta} \rangle + \epsilon_k, \quad (3.2)$$

i.i.d. ϵ_k are viewed as 3-dimensional real vectors and further assumed to obey multivariate Gaussian distribution $\mathcal{N}(0, \Sigma_c)$. We study the problem of recovering $\tilde{\Theta}$ via the data $\{(\mathbf{X}_k, Y_k) : k \in [n]\}$. Since \mathbf{X}_k are i.i.d. distributed, one position may be observed twice or even more in our model, while existing work (e.g., [16, 24, 28]) considered sampling without replacement (where one entry is either observed once or unknown), which seems quite different from our problem set-up. But it has been showed that under the same observation number, sampling without replacement is at least as good as sampling with replacement [17], which is obvious in the clean model (3.1) since observing one position twice doesn't provide more information. In brief, we are indeed coping with more difficult sampling scheme, hence our results manage to support their problem settings.

We first consider the clean case without noise (3.1). Our method requires a prior estimation of the max norm

$$\|\tilde{\Theta}\|_{\infty} \leq \alpha. \quad (3.3)$$

Since the gray value is smaller than 255, α can always be $255\sqrt{3}$, but a tighter bound on $\|\tilde{\Theta}\|_{\infty}$ would be preferable and bring higher inpainting quality. The precise observations are used as constraints, by combining with (3.3) we complete the color image via minimizing the nuclear norm,

$$\hat{\Theta} \in \arg \min_{\Theta \in \mathbb{Q}_{\text{pix}}^{d_1 \times d_2}} \|\Theta\|_{\text{nu}}, \text{ s.t. } \|\Theta\|_{\infty} \leq \alpha, \langle \mathbf{X}_k, \Theta \rangle = Y_k, k \in [n]. \quad (3.4)$$

In (3.2) the observations are corrupted and not completely reliable, so we use a weighted quadratic loss to fit the observed data:

$$\mathcal{L}_w(\Theta) = \frac{1}{2n} \sum_{k=1}^n |Y_k - \langle \mathbf{X}_k, \Theta \rangle|_w^2, \quad \Theta \in \mathbb{Q}_{\text{pix}}^{d_1 \times d_2}. \quad (3.5)$$

To avoid scaling confusion we assume $\text{Tr } \mathbf{W} = \|\mathbf{W}\|_{\text{nu}} = \sum_i \lambda_i(\mathbf{W}) = 3$, which means assigning a total weight 3 to three channels for diagonal \mathbf{W} , and note that when $\mathbf{W} = \mathbf{I}_3$ (3.5) reduces to the commonly used quadratic loss [13, 22, 29, 31, 53]. In accordance to the weight \mathbf{W} we require a prior estimation on the weighted max norm

$$\|\tilde{\Theta}\|_{w,\infty} \leq \alpha. \quad (3.6)$$

Let the nuclear norm serve as regularizer that promote low-rankness, and λ be the tuning parameter to balance the loss and regularization, the inpaint method is formulated as

$$\hat{\Theta} \in \arg \min_{\Theta \in \mathbb{Q}_{\text{pix}}^{d_1 \times d_2}} \mathcal{L}_w(\Theta) + \lambda \|\Theta\|_{\text{nu}}, \quad \text{s.t. } \|\Theta\|_{w,\infty} \leq \alpha. \quad (3.7)$$

Although natural image is believed to contain high redundancies, it need not to be exactly low-rank. To be more practical, we assume $\tilde{\Theta}$ to be approximately low-rank under a specific $0 \leq q < 1$:

$$\sum_{i=1}^{\min\{d_1, d_2\}} |\sigma_i(\tilde{\Theta})|^q \leq \rho, \quad (3.8)$$

which reduces to low-rank when $q = 0$.

3.1 Error Bound

Let $\hat{\Delta} = \hat{\Theta} - \tilde{\Theta}$ be the reconstructed error, in this part we bound $\|\hat{\Delta}\|_F$ for (3.1), (3.2). Different from matrix sensing that has an elegant theory parallel to compressed sensing [5], it is challenging to establish restricted isometry property (RIP) without incoherence condition in matrix completion [15]. To replace RIP, [33] first established the restricted strong convexity (RSC) over a constraint set and obtained an error bound, but the quite lengthy and intricate proof therein involves construction of δ -net, Sudakov minoration, and so forth. By considering a different constraint set, [25] successfully refined the proof for exact low-rank situation.

Also, the RSC of $\mathcal{L}_w(\Theta)$ presented in Lemma 5 plays a crucial role in our proof. As technical contribution, Lemma 5 not only extends [25] to quaternion, but also extends to approximately low-rank situation, which owes to a tricky modification of the critical constraint set, see (3.9). We mention that the second extension may be of interest even if reduced to traditional real matrix completion, e.g., it provides an alternative and simpler proof of the main result in [33].

Lemma 5. *Consider the constraint set with parameter $\psi = (\psi_1, \psi_2, \psi_3)$ where ψ_3 is slightly large*

$$\begin{aligned} \mathcal{C}(\psi) = \left\{ \Theta \in \mathbb{Q}_{\text{pure}}^{d_1 \times d_2} : \|\Theta\|_{w,\infty} \leq \psi_1 \alpha, \|\Theta\|_{\text{nu}} \leq \psi_2 \rho^{\frac{1}{2-q}} \|\Theta\|_F^{\frac{2-2q}{2-q}}, \right. \\ \left. \|\Theta\|_{w,F}^2 \geq \alpha^2 d_1 d_2 \sqrt{\frac{\psi_3 \log(d_1 + d_2)}{n}} \right\}. \end{aligned} \quad (3.9)$$

Let $\mathcal{X} = (\mathbf{X}_1, \dots, \mathbf{X}_n)$, $\Theta \in \mathbb{Q}_{\text{pure}}^{d_1 \times d_2}$, we define

$$\mathcal{F}_{\mathcal{X}}(\Theta) = \frac{1}{n} \sum_{k=1}^n |\langle \mathbf{X}_k, \Theta \rangle|_{\text{w}}^2. \quad (3.10)$$

Then there exists constant $\kappa \in (0, 1)$ such that with probability at least $1 - 2(d_1 + d_2)^{-3/4}$, for all $\Theta \in \mathcal{C}(\psi)$ it holds that

$$\mathcal{F}_{\mathcal{X}}(\Theta) \geq \frac{\kappa}{d_1 d_2} \|\Theta\|_{\text{w}, \text{F}}^2 - T_0, \quad (3.11)$$

where the relaxation term T_0 is given by

$$T_0 = \frac{\rho}{(2-q)(\sqrt{d_1 d_2})^q} \left(36\psi_1\psi_2\alpha \frac{\|\mathbf{W}\|_{\infty}^{1/2}}{\lambda_{\min}(\sqrt{\mathbf{W}})} \sqrt{\frac{\max\{d_1, d_2\} \log(d_1 + d_2)}{n}} \right)^{2-q}. \quad (3.12)$$

The core idea of the proof is to discuss whether the error $\widehat{\Delta}$ falls in $\mathcal{C}(\psi)$, which helps unfold some key relations that further lead to an error bound. By (3.3), (3.6), it is straightforward that $\widehat{\Delta}$ satisfies the first constraint in (3.9). In Lemma 6 we show that in both clean and corrupted cases, the error satisfies the second constraints for certain ψ_2 . The proof relies on analysis of a pair of subspace $(\mathcal{M}, \overline{\mathcal{M}})$ over which the nuclear norm is decomposable, see a unified framework in [34].

Lemma 6. *Assume (3.8) holds.*

(1) *In the clean model (3.1) with prior estimation (3.3), we recover $\widetilde{\Theta}$ via (3.4), then we have*

$$\|\widehat{\Delta}\|_{\text{nu}} \leq 5\rho^{\frac{1}{2-q}} \|\widehat{\Delta}\|_{\text{F}}^{\frac{2-2q}{2-q}}. \quad (3.13)$$

(2) *In the corrupted model (3.2) with prior estimation (3.6), we recover $\widetilde{\Theta}$ via (3.7) with the weighted loss in (3.5). If for some $C_1 > 1$, λ satisfies*

$$\lambda \geq C_1 \left\| \frac{1}{n} \sum_{k=1}^n (\mathbf{W} \boldsymbol{\epsilon}_k) \mathbf{X}_k \right\|_{\text{op}} \quad (3.14)$$

then we have

$$\|\widehat{\Delta}\|_{\text{nu}} \leq \frac{5C_1}{C_1 - 1} \rho^{\frac{1}{2-q}} \|\widehat{\Delta}\|_{\text{F}}^{\frac{2-2q}{2-q}}. \quad (3.15)$$

With the aid of Lemma 5, Lemma 6, we are now in a position to derive error bound of the clean model (3.1). We give an upper bound on the mean square error (MSE), i.e., $\|\widehat{\Delta}\|_{\text{F}}^2/(d_1 d_2)$, which directly links to the commonly used peak signal-to-noise ratio (PSNR), or the Frobenius norm error $\|\widehat{\Delta}\|_{\text{F}}$.

Theorem 1. *Consider the clean model (3.1) with prior estimation (3.3), the color image is reconstructed by (3.4). Assume the original image satisfies (3.8). If $n < d_1 d_2$, $\rho \gtrsim (d_1 d_2)^{q/2}$, $\max\{d_1, d_2\} \log(d_1 + d_2)/n$ is sufficiently small, the error bound for MSE holds*

$$\frac{\|\widehat{\Delta}\|_{\text{F}}^2}{d_1 d_2} \lesssim \frac{\rho}{(d_1 d_2)^{q/2}} \left(\alpha^2 \frac{\max\{d_1, d_2\} \log(d_1 + d_2)}{n} \right)^{1-q/2} \quad (3.16)$$

with probability at least $1 - 2(d_1 + d_2)^{-3/4}$.

Remark 2. From (3.16), sampling complexity $n = O(\max\{d_1, d_2\} \log(d_1 + d_2))$ suffices to guarantee a small MSE, but it may not be exciting enough since MSE is a more element-wise notion. To be more insightful, we rewrite (3.16) to be a bound of relative square error (RSE):

$$\frac{\|\widehat{\Delta}\|_{\text{F}}^2}{\|\widetilde{\Theta}\|_{\text{F}}^2} \lesssim \frac{\rho}{\|\widetilde{\Theta}\|_{\text{F}}^q} \left(\alpha(\widetilde{\Theta})^2 \frac{\max\{d_1, d_2\} \log(d_1 + d_2)}{n} \right)^{1-q/2}, \quad (3.17)$$

where $\alpha(\widetilde{\Theta})$ given by

$$\alpha(\widetilde{\Theta}) = \frac{\sqrt{d_1 d_2} \|\widetilde{\Theta}\|_{\infty}}{\|\widetilde{\Theta}\|_{\text{F}}} \in [1, \sqrt{d_1 d_2}]$$

is known as the spikiness of $\widetilde{\Theta}$, which was first proposed in [33] for a real matrix. Therefore, a small RSE can be guaranteed under $n = O(\max\{d_1, d_2\} \log(d_1 + d_2))$ for $\widetilde{\Theta}$ with spikiness close to 1. Note that natural (color) images tend to be smooth locally [3] and contains similar patches globally [14], so they are supposed to have low spikiness, which can also be verified effortlessly. In comparison, the exact recovery framework in [24] cannot fit natural images well due to the unrealistic "incoherence" assumption, which is more stringent than low spikiness [33].

For the corrupted case we need Lemma 7 to give instruction on tuning the λ , which is expected to satisfy (3.14) so that (3.15) holds. After all these preparations, in Theorem 2 we establish an error bound under general Gaussian noise and a general weighted loss, by similar methodology.

Lemma 7. In (3.7) if we choose

$$\lambda = 2C_1 \sqrt{\frac{\text{Tr}(\mathbf{W} \Sigma_c \mathbf{W}) \log(d_1 + d_2)}{n \min\{d_1, d_2\}}}, \quad (3.18)$$

then (3.14) holds with probability higher than $1 - 4(d_1 + d_2)^{-3/4}$.

Theorem 2. Consider the corrupted model (3.2) where $\epsilon_k \sim \mathcal{N}(0, \Sigma_c)$, given the positive definite weight \mathbf{W} satisfying $\text{Tr} \mathbf{W} = 3$, we have the prior estimation (3.6). Assume the original image satisfies (3.8). We reconstruct the color image via (3.7) where the loss function is given in (3.5). We choose λ by (3.18). If $n < d_1 d_2$, $\rho \gtrsim (d_1 d_2)^{q/2}$, $\max\{d_1, d_2\} \log(d_1 + d_2)/n$ is small, then with probability at least $1 - 6(d_1 + d_2)^{-3/4}$ we have the error bound for MSE

$$\frac{\|\widehat{\Delta}\|_{\text{F}}^2}{d_1 d_2} \lesssim \frac{\rho}{(d_1 d_2)^{q/2}} \left(\max \left\{ \frac{\|\mathbf{W}\|_{\infty} \alpha^2}{\lambda_{\min}(\mathbf{W})^3}, \frac{\text{Tr}(\mathbf{W} \Sigma_c \mathbf{W})}{\lambda_{\min}(\mathbf{W})^2} \right\} \frac{\max\{d_1, d_2\} \log(d_1 + d_2)}{n} \right)^{1-q/2}. \quad (3.19)$$

3.2 Noise Correction

Due to the i.i.d. Gaussian noise that corrupts each observation, we are required to conduct completion and denoising simultaneously when we cope with the robust completion problem. How to model and then handle cross-channel noise has been noted to be an important issue in color image denoising [32, 48], thus, a careful treatment for the noise is also necessary in our robust inpainting problem (3.2). Motivated by the obtained error bound (3.19), we propose

to use a cross-channel weight \mathbf{W} to handle unbalanced or highly correlated noise, which is referred to be a noise correction strategy.

Compared with the bound of clean model (3.16), the bound under corrupted observations contains two extra factors involving the noise covariance matrix Σ_c and the cross-channel weight \mathbf{W} , i.e.,

$$F_1 = \frac{\|\mathbf{W}\|_\infty}{\lambda_{\min}(\mathbf{W})^3} \quad \text{and} \quad F_2 = \frac{\text{Tr}(\mathbf{W}\Sigma_c\mathbf{W})}{\lambda_{\min}(\mathbf{W})^2}.$$

Under assumption $\text{Tr}(\mathbf{W}) = 3$, it can be easily verified that $\|\mathbf{W}\|_\infty \geq 1$, $\lambda_{\min}(\mathbf{W}) \leq 1$, for both inequalities the equal sign holds if and only if $\mathbf{W} = \mathbf{I}_3$, meaning that the error bound becomes worse when \mathbf{W} deviates from \mathbf{I}_3 . The guideline that \mathbf{W} should not be far away from the identity matrix is mainly because the non-weighted loss (i.e., $\mathbf{W} = \mathbf{I}_3$) best fits the square error (or MSE, RSE, PSNR) that we care about. On the other hand, the numerator of F_2 , $\text{Tr}(\mathbf{W}\Sigma_c\mathbf{W})$, seems to indicate an appropriate weight for the noise.

3.2.1 Noise Level Rebalance

In some applications some prior knowledge on noise levels is available, also some efficient methods to estimate noise variance in image data have been developed [12, 27]. We assume the diagonal of Σ_c is known to be $[\sigma_r^2, \sigma_g^2, \sigma_b^2]^T$. In the corrupted model, a noise with remarkably different $\sigma_r^2, \sigma_g^2, \sigma_b^2$ could be problematic, since the observations in three channels have different data fidelities. More precisely, data in the channel suffering from severer noise will be less reliable than those in low noise channel.

To deal with the issue of data fidelity, we use a diagonal $\mathbf{W} = \text{diag}(w_r, w_g, w_b)$ that assign higher weight to channel with more precise data, to rebalance the noise level. It is not hard to show that

$$\mathbf{W}_s = \frac{3\text{diag}(\sigma_r^{-2}, \sigma_g^{-2}, \sigma_b^{-2})}{\sigma_r^{-2} + \sigma_g^{-2} + \sigma_b^{-2}} \quad (3.20)$$

is the only diagonal matrix minimizing $\text{Tr}(\mathbf{W}\Sigma_c\mathbf{W})$. Except for the motivation from the bound, such a choice can also be justified by a simple reasoning. Note that (3.2) is equivalent to

$$\sqrt{\mathbf{W}_s}Y_k = \langle \mathbf{X}_k, \sqrt{\mathbf{W}_s}\tilde{\Theta} \rangle + \sqrt{\mathbf{W}_s}\epsilon_k, \quad (3.21)$$

and $\sqrt{\mathbf{W}_s}\epsilon_k$ have equal noise levels, so data in three channels of $\sqrt{\mathbf{W}_s}\tilde{\Theta}$ have equal data fidelity, therefore, a fair loss would be

$$\begin{aligned} & \frac{1}{2n} \sum_{k=1}^n |\sqrt{\mathbf{W}_s}Y_k - \langle \mathbf{X}_k, \sqrt{\mathbf{W}_s}\Theta \rangle|^2 \\ &= \frac{1}{2n} \sum_{k=1}^n |\sqrt{\mathbf{W}_s}(Y_k - \langle \mathbf{X}_k, \Theta \rangle)|^2 \\ &= \mathcal{L}_{\mathbf{W}_s}(\Theta). \end{aligned}$$

In summary, on one hand, \mathbf{W} cannot deviate much from \mathbf{I}_3 to maintain the alignment of the loss $\mathcal{L}_w(\Theta)$ and the considered square error $\|\hat{\Delta}\|_F^2$; on the other hand, \mathbf{W} close to \mathbf{W}_s is preferred thanks to its ability to rebalance noise levels. As a trade-off, our proposal is to use the convex combination

$$\mathbf{W}(\gamma) = (1 - \gamma)\mathbf{I}_3 + \gamma\mathbf{W}_s, \quad (3.22)$$

where $\gamma \in [0, 1]$.

We mention that the idea of handling unbalanced noise via weighting three channels was first proposed in Jun Xu et al. [48], but it worked on denoising which is different from our robust inpainting problem. More importantly, they failed to see the requirement that the weight cannot go far away from the identity matrix, and set the weight to be $\mathbf{W}(1) = \mathbf{W}_s$. We will use experimental results to show that a proper γ in (3.22) is crucial, while the extreme choice $\mathbf{W}(1) = \mathbf{W}_s$ seems inadvisable, and could even lead to degraded result worse than a non-weighted loss $\mathbf{W}(0) = \mathbf{I}_3$.

3.2.2 Noise Correlation Removal

Although noise of different scales has been considered in [48], few work studied correlated noise in color images, e.g., [48] assumed noises in three channels are independent. In this part, we report that highly-correlated noise could also be detrimental, probably because such noise introduces extra cross-channel correlations that mixes with the original RGB couplings, making it more difficult to recognize the underlying color image. Then, we propose to use a positive definite weight \mathbf{W} to remove (some) correlations of the noise. To focus on the strategy *per se*, we assume we have full knowledge of Σ_c , and select a \mathbf{W} that minimize $\text{Tr}(\mathbf{W}\Sigma_c\mathbf{W})$.

Lemma 8. *Under the assumption $\text{Tr } \mathbf{W} = 3$, and \mathbf{W} is positive definite. Then*

$$\mathbf{W}_c = \frac{3\Sigma_c^{-1}}{\text{Tr}(\Sigma_c^{-1})} \quad (3.23)$$

is the unique weight that minimizes $\text{Tr}(\mathbf{W}\Sigma_c\mathbf{W})$.

In analogy, the advantage of (3.23) can also be seen by transforming the model as (3.21), and note that $\sqrt{\mathbf{W}_c}\epsilon_k \sim \mathcal{N}(0, 3\mathbf{I}_3/\text{Tr}(\Sigma_c^{-1}))$. As a trade-off among \mathbf{I}_3 , \mathbf{W}_s and \mathbf{W}_c , we propose to choose \mathbf{W} by

$$\mathbf{W}(\gamma_1, \gamma_2) = (1 - \gamma_1 - \gamma_2)\mathbf{I}_3 + \gamma_1\mathbf{W}_s + \gamma_2\mathbf{W}_c, \quad (3.24)$$

where $\gamma_1 > 0$, $\gamma_2 > 0$, $\gamma_1 + \gamma_2 \leq 1$. When the noise correlations are benign, or Σ_c is unknown, we simply let $\gamma_2 = 0$, then (3.24) reduces to our previous proposal (3.22).

4 Numerical Study

4.1 Algorithms

By virtue of the convexity, we apply ADMM [4] to solve both (3.4) and (3.7). During the iteration, quaternion with non-zero real part may occur, and we allow $\mathbf{W} \in \mathbb{R}^{3 \times 3}$ to operate on the quaternion by simply operating on the imaginary part, i.e., $\mathbf{W}\mathbf{q} = \text{Re}\mathbf{q} + \mathbf{W}\text{Im}\mathbf{q}$. We let $\mathbf{W}(\cdot)$, $\text{Re}(\cdot)$, $\text{Im}(\cdot)$ element-wisely operate on a quaternion matrix. We introduce the singular values soft thresholding operator \mathcal{S}_τ for $\mathbf{A} \in \mathbb{Q}^{d_1 \times d_2}$, which is used in solving the subproblem. Calculate the QSVD $\mathbf{A} = \mathbf{U}\Sigma\mathbf{V}^*$ where $\Sigma = \text{diag}(\sigma_1, \dots, \sigma_{\min\{d_1, d_2\}}) \in \mathbb{R}^{d_1 \times d_2}$, then define $\mathcal{S}_\tau(\mathbf{A}) = \mathbf{U}\mathcal{S}_\tau(\Sigma)\mathbf{V}^*$, where $\mathcal{S}_\tau(\cdot)$ element-wisely operates on Σ (recall that $\mathcal{S}_\tau(a) = \text{sign}(a) \max\{|a| - \tau, 0\}$ for $a \in \mathbb{R}$). Besides, let $\mathbb{1}(\mathcal{E})$ be the indicator function of event \mathcal{E} , i.e., $\mathbb{1}(\mathcal{E}) = 0$ if \mathcal{E} happens, otherwise, $\mathbb{1}(\mathcal{E}) = \infty$.

For clean model (3.1), we use $\Omega \subset [d_1] \times [d_2]$ to denote the set of observed positions. In corrupted model (3.4) we assume the (i,j) position is observed $n(i, j)$ times in total, with the observed values being $\mathbf{y}_{(i,j),k}$, $1 \leq k \leq n(i, j)$. We define $\mathbf{J}_1 \in \mathbb{Q}^{d_1 \times d_2}$ whose (i,j)-entry is $\sum_{k=1}^{n(i,j)} \mathbf{y}_{(i,j),k}$, and let $\mathbf{J}_2 \in \mathbb{N}^{d_1 \times d_2}$ with $n(i, j)$ as the (i,j)-entry. We define constraint sets

$$\begin{cases} \Omega_1 = \{[\mathbf{a}_{ij}] \in \mathbb{Q}_{\text{pix}}^{d_1 \times d_2} : |\mathbf{a}_{ij}| \leq \alpha, \forall (i, j); \mathbf{a}_{ij} = \tilde{\theta}_{ij}, \forall (i, j) \in \Omega\} \\ \Omega_2 = \{[\mathbf{a}_{ij}] \in \mathbb{Q}^{d_1 \times d_2} : \text{Re} \mathbf{a}_{ij} = 0, |\mathbf{a}_{ij}| \leq \alpha, \forall (i, j)\} \end{cases}.$$

Note that (3.4) is equivalent to

$$\arg \min_{\mathbf{X}, \mathbf{Z}} \mathbb{1}(\mathbf{X} \in \Omega_1) + \|\mathbf{Z}\|_{\text{nu}}, \text{ s.t. } \mathbf{X} = \mathbf{Z},$$

by a standard ADMM, we obtain the iterative formula

$$\begin{cases} \mathbf{X}^{t+1} = \mathcal{P}_{\Omega_1}(\mathbf{Z}^t - \mathbf{\Lambda}^t / \rho) \\ \mathbf{Y}^{t+1} = \mathcal{S}_{1/\rho}(\mathbf{X}^{t+1} + \mathbf{\Lambda}^t / \rho) \\ \mathbf{\Lambda}^{t+1} = \mathbf{\Lambda}^t + \rho(\mathbf{X}^{t+1} - \mathbf{Z}^{t+1}) \end{cases}. \quad (4.1)$$

Sufficiently small $\|\mathbf{X}^t - \mathbf{Z}^t\|_{\text{F}}$ is used as the stopping criterion.

For positive definite \mathbf{W} (3.7) can be recast as (let $\Omega_3 = \mathbb{Q}_{\text{pix}}^{d_1 \times d_2}$)

$$\begin{aligned} \arg \min_{\mathbf{X}_{(i)}, \mathbf{Z}} \frac{1}{2n} \sum_{k=1}^n |\sqrt{\mathbf{W}} Y_k - \langle \mathbf{X}_k, \mathbf{X}_{(1)} \rangle|^2 + \mathbb{1}(\mathbf{X}_{(1)} \in \Omega_2) + \lambda \|\mathbf{X}_{(2)}\|_{\text{nu}} \\ + \mathbb{1}(\mathbf{X}_{(3)} \in \Omega_3) + \mathbb{1}(\text{Re} \mathbf{Z} = 0), \text{ s.t. } \mathbf{X}_{(1)} = \sqrt{\mathbf{W}} \mathbf{Z}, \mathbf{X}_{(2)} = \mathbf{X}_{(3)} = \mathbf{Z}. \end{aligned}$$

Similarly, some deductions give the algorithm as

$$\begin{cases} \mathbf{X}_{(1)}^{t+1} = \mathcal{P}_{\Omega_2}(\{n\rho\sqrt{\mathbf{W}} \mathbf{Z}^t + \sqrt{\mathbf{W}} \mathbf{J}_1 - n\mathbf{\Lambda}_{(1)}^t\} ./ \{n\rho\mathbf{1} + \mathbf{J}_2\}) \\ \mathbf{X}_{(2)}^{t+1} = \mathcal{S}_{\lambda/\rho}(\mathbf{Z}^t - \rho^{-1} \mathbf{\Lambda}_{(2)}^t) \\ \mathbf{X}_{(3)}^{t+1} = \mathcal{P}_{\Omega_3}(\mathbf{Z}^t - \rho^{-1} \mathbf{\Lambda}_{(3)}^t) \\ \mathbf{Z}^{t+1} = \text{Im}(\{2\mathbf{I}_3 + \mathbf{W}\}^{-1} \{ \sqrt{\mathbf{W}}(\mathbf{X}_{(1)}^{t+1} + \rho^{-1} \mathbf{\Lambda}_{(1)}^t) \\ + \mathbf{X}_{(2)}^{t+1} + \rho^{-1} \mathbf{\Lambda}_{(2)}^t + \mathbf{X}_{(3)}^{t+1} + \rho^{-1} \mathbf{\Lambda}_{(3)}^t \}) \\ \mathbf{\Lambda}_{(1)}^{t+1} = \mathbf{\Lambda}_{(1)}^t + \rho(\mathbf{X}_{(1)}^{t+1} - \sqrt{\mathbf{W}} \mathbf{Z}^{t+1}) \\ \mathbf{\Lambda}_{(2)}^{t+1} = \mathbf{\Lambda}_{(2)}^t + \rho(\mathbf{X}_{(2)}^{t+1} - \mathbf{Z}^{t+1}) \\ \mathbf{\Lambda}_{(3)}^{t+1} = \mathbf{\Lambda}_{(3)}^t + \rho(\mathbf{X}_{(3)}^{t+1} - \mathbf{Z}^{t+1}) \end{cases}, \quad (4.2)$$

and we use " $\|\mathbf{X}_{(1)}^t - \sqrt{\mathbf{W}} \mathbf{Z}^t\|_{\text{F}} + \|\mathbf{X}_{(2)}^t - \mathbf{Z}^t\|_{\text{F}} + \|\mathbf{X}_{(3)}^t - \mathbf{Z}^t\|_{\text{F}}$ is sufficiently small" as the stopping criterion.

In (4.1), (4.2), ". /" is the elementwise division, $\mathbf{1}$ is the all-ones matrix, $\mathbf{\Lambda}, \mathbf{\Lambda}_{(i)}$ is the multipliers, ρ is the parameter in the augmented Lagrangian function, $\mathcal{P}_{\Omega_i}(\cdot)$ is the projection with respect to Frobenius norm. Note that all the projections used have closed form solutions.

It is worthy to mention that the number of variables in (4.2) can be reduced when \mathbf{W} is diagonal, and we do use the simplified algorithm in the experiments. Besides, both (4.1), (4.2) are 2-block ADMM in essence, hence the convergence is guaranteed [18].

4.2 Synthetic Data

In this part we generate synthetic (approximately) low-rank non-negative pure quaternion matrix (NNPQM) for numerical simulations, aiming to illustrate the relations in the obtained error bound and verify the effectiveness of the proposed noise correction strategy. Also we compare observation with or without replacement.

For exact low-rank NNPQM (3.16) reads

$$\text{MSE} \lesssim \alpha^2 \text{rank}(\tilde{\Theta}) \frac{\max\{d_1, d_2\} \log(d_1 + d_2)}{n}, \quad (4.3)$$

To confirm the relations among MSE, n , rank and dimension of underlying matrix, we generate square NNPQMs with different rank r and dimension d , and α about the same. MSE for each matrix under a specific n is set as the mean value of 10 repetitions. The plots of "MSE v.s. n " for synthetic NNPQM with " $r = 50, d = 15$ ", " $r = 70, d = 15$ ", " $r = 70, d = 20$ ", " $r = 90, d = 20$ " are showed in Figure 1. We can see that the curves in the left figure shift to the right with larger d or r , since more observations are needed to complete a quaternion matrix of larger size or higher rank. Consistent with (4.3), the plots of "MSE v.s. the rescaled sample size $n/(rd \log 2d)$ " roughly fall in the same position, meaning that the relation between MSE and n mainly relies on r and d .

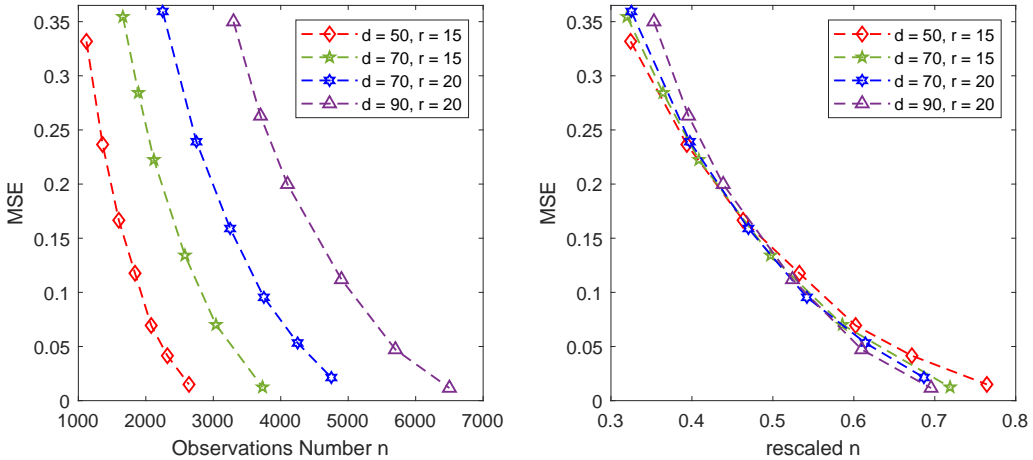


Figure 1: $q = 0$, MSE v.s. n or $\frac{n}{rd \log(2d)}$ under different d, r

The approximate low-rank case under (3.8) with $q = \frac{1}{2}$ is also numerically simulated. We generate NNPQM of size 50×50 , 70×70 , 90×90 , all are of full rank but only a few singular values are significant. Both "MSE v.s. n " and "MSE v.s. rescaled n " match (3.16) fairly well, see Figure 2.

In Remark 2 we show that the relative square error (RSE) is also related to the spikiness of the underlying NNPQM, this fact can be clearly seen under the most spiky NNPQM that has only one nonzero entry, since such a matrix cannot be well estimated with incomplete observations [15]. To further illustrate the relation between RSE and spikiness, we generate 50×50 rank-20 NNPQMs with different spikiness, then obtain the RSE (set as mean value of 15 repetitions) of each matrix under different n . As expected, the NNPQM with lower spikiness can be better estimated. We mention that hundreds of color images tested in our numerical study have spikiness lower than 2 (see Remark 2 for underlying rationale), thus, our framework nicely embraces color images.

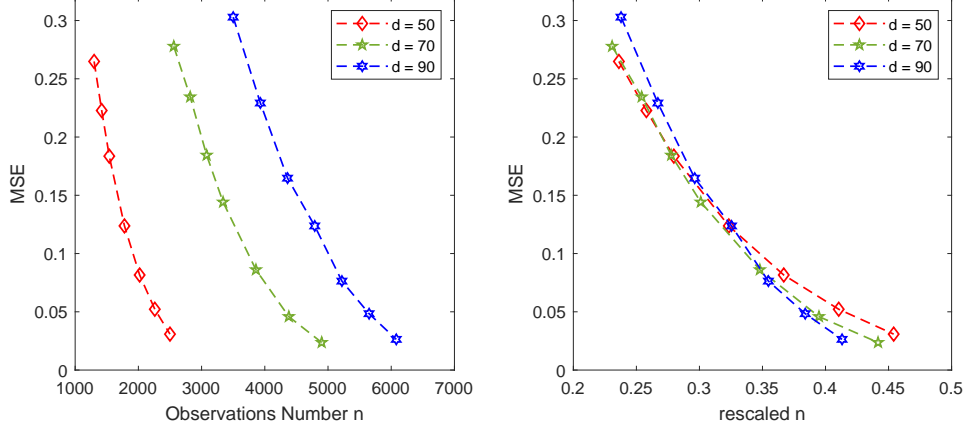


Figure 2: $q = \frac{1}{2}$, MSE v.s. n or $\frac{n}{(\rho d^{-q})^{2/(2-q)} d \log(2d)}$ under different d, ρ

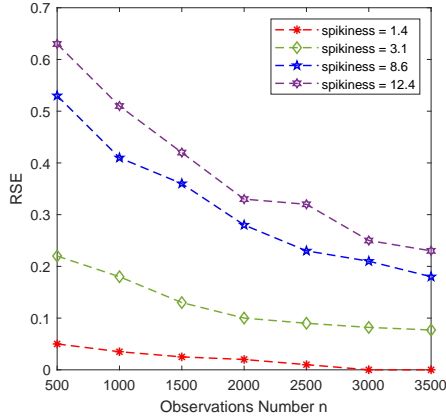


Figure 3: RSE v.s. n , under different spikiness, the same d, r

It has been showed in [17] that no-replacement sampling is at least as good as sampling with replacement used in (3.1), (3.2). As a double check we compare two sampling schemes on a fixed 30×30 rank-5 NNPQM under the corrupted model with different noise scales. From the results showed in Figure 4, sampling without replacement seems more informative and leads to smaller error under the same conditions. In the following experiments, we switch to sampling without replacement since it is aligned with more real problems.

Recall that we propose to deal with unbalanced or correlated noise via choosing a suitable cross-channel weight, including noise level rebalance and noise correlation removal, see (3.22), (3.24) for the precise proposals. We first confirm the efficacy of "rebalancing noise level" on a synthetic 30×30 rank-5 NNPQM, whose entries are corrupted by i.i.d. unbalanced Gaussian noise with covariance matrix $\Sigma_c = \text{diag}(1.5, 0.5, 0.2)$. By (3.20) the weight that completely achieves equal data fidelity is $\mathbf{W}_s = \text{diag}(2/9, 10/9, 5/3)$, so we use

$$\mathbf{W}(\gamma) = \text{diag}([1 - \frac{7}{9}\gamma, 1 + \frac{1}{9}\gamma, 1 + \frac{2}{3}\gamma])$$

as a trade-off. In the experiment we examined $\gamma = 0, 0.2, 0.4, 0.6, 0.8, 1.0$, where $\gamma = 0$ becomes the non-weighted case, and $\gamma = 1$ corresponds to the proposal in [48]. Note that a

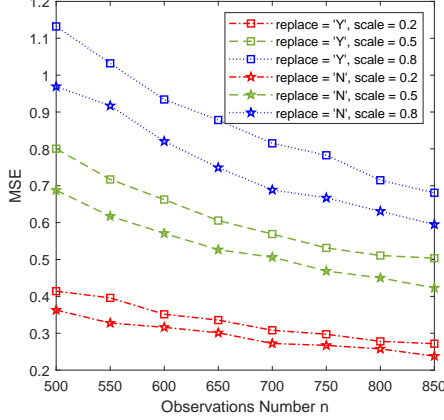


Figure 4: MSE v.s. n under different noise levels (scales), $replace = 'Y'$ or $'N'$ stands for sampling with or without replacement, respectively.

proper scaling of λ in (3.7) is provided in (3.18), thus, we set

$$\lambda = C(\lambda) \sqrt{\frac{\text{Tr}(\mathbf{W}\Sigma_c\mathbf{W}) \log(2d)}{nd}} \quad (4.4)$$

for specific \mathbf{W} . $C(\lambda)$ is tuned to (nearly) optimal for a fair comparison among different $\mathbf{W}(\gamma)$, and in this simulation the optimal $C(\lambda)$ always lies between 0.4 and 0.8. In Figure 5 we show the results under sample size 900, 800, 700, 500, when "n = 900" the robust completion problem becomes a standard denoising problem (recall that we sample without replacement).

From Figure 5, we see that a properly weighted loss brings significant improvement: When n equals 900 or 800, the curves of $\mathbf{W}(0.2)$, $\mathbf{W}(0.4)$, $\mathbf{W}(0.6)$ uniformly lie below that of $\mathbf{W}(0)$; When n equals 700, 500, the minimum MSE of $\mathbf{W}(0.4)$ or $\mathbf{W}(0.6)$ is still notably smaller compared with the non-weighted loss. It is interesting to see that a full balance of noise level, i.e., $\mathbf{W}(1) = \mathbf{W}_s$, is not a wise choice, since it results in severe degradation.

In analogy we show removing noise correlation is an effective strategy to deal with correlated noise. We generate a 30×30 rank-2 NNPQM and then corrupt its entries by i.i.d. 3-dimensional Gaussian noise, which is highly, positively correlated with covariance matrix

$$\Sigma_c = \begin{bmatrix} 0.70 & 0.50 & 0.50 \\ 0.50 & 0.70 & 0.66 \\ 0.50 & 0.66 & 0.70 \end{bmatrix}.$$

Note that noise levels in three channels are the same, hence $\mathbf{W}_s = \mathbf{I}_3$, and (3.24) reduces to

$$\mathbf{W}(\gamma) = (1 - \gamma)\mathbf{I}_3 + \gamma\mathbf{W}_c, \quad (4.5)$$

where \mathbf{W}_c is determined by (3.23). Similarly we test $\gamma = 0, 0.2, 0.4, 0.6, 0.8, 1.0$ under $n = 900$ (denoising), 700, 400, 200. λ is set as (4.4) where $C(\lambda)$ is well tuned. The experimental results are showed in Figure 6.

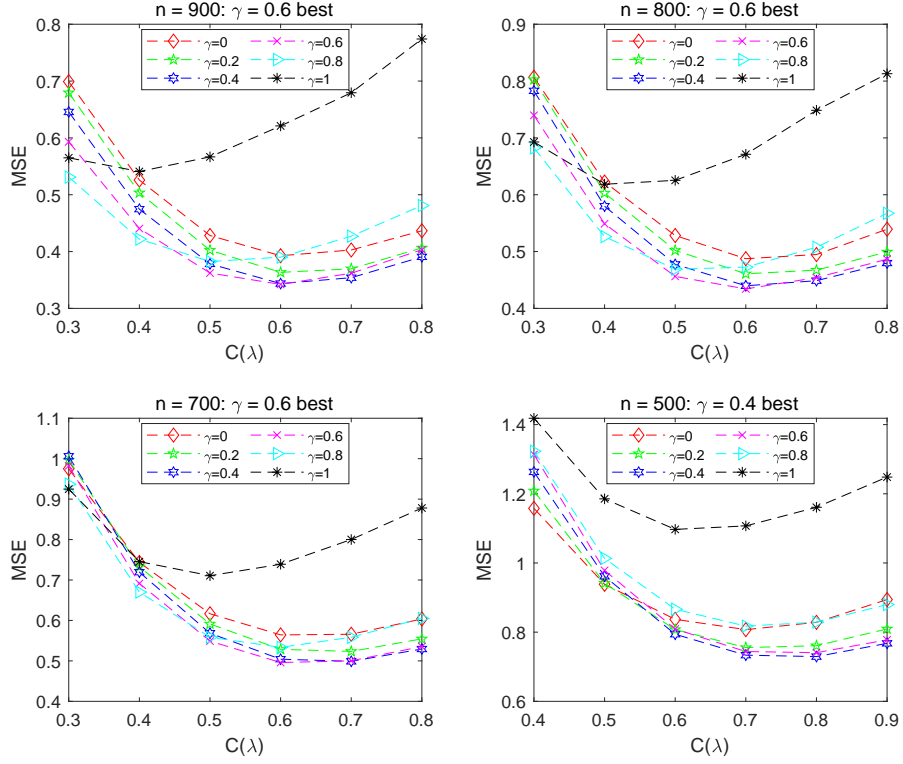


Figure 5: (Noise level rebalance) MSE v.s. $C(\lambda)$ for $\gamma = 0, 0.2, 0.4, 0.6, 0.8, 1$, under $n = 900, 800, 700, 500$. The best γ corresponding to the smallest MSE is given in the title.

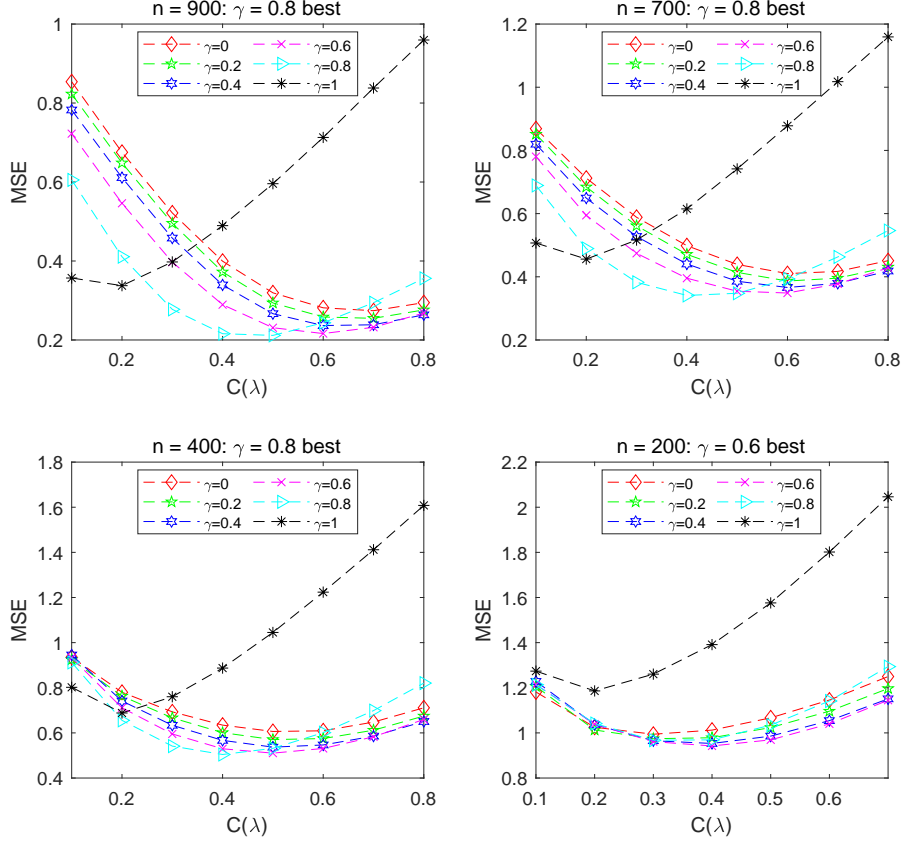


Figure 6: (Noise correlation removal) MSE v.s. $C(\lambda)$ for $\gamma = 0, 0.2, 0.4, 0.6, 0.8, 1$, under $n = 900, 700, 400, 200$. The best γ corresponding to the smallest MSE is given in the title.

In denoising and robust completion with sample size 700 or 400, $\mathbf{W}(0.2)$, $\mathbf{W}(0.4)$, $\mathbf{W}(0.6)$ are uniformly better than a non-weighted loss, while $\mathbf{W}(0.8)$ achieves the smallest square error. In a situation where less observations are available ($n = 200$), the minimum MSE achieved by " $\gamma = 0.6$ " notably improves that of " $\gamma = 0$ ". In addition, using $\mathbf{W}(1) = \mathbf{W}_c$ that removes all correlations of noise leads to result worse than non-weighted loss, since it deviates from the identity matrix too much.

Remark 3. *This remark is intended to provide an insight of γ . Since each observation is corrupted by noise in (3.2), the robust completion problem can be viewed as a combination of completion and denoising. The only purpose of using \mathbf{W}_s or \mathbf{W}_c in $\mathbf{W}(\gamma)$ is to adjust to the noise pattern and facilitate the denoising. By contrast, the other component \mathbf{I}_3 aims to achieve the alignment between loss function and square error, hence it is crucial for the whole problem. From this perspective, γ is actually weighting "to what extent the robust completion is a denoising problem". It is interesting to note that in Figure 5, Figure 6 when n becomes smaller, the optimal γ moves towards 0, and the curves of different γ become closer, indicating that the improvement is less significant. This is because the completion dominates the whole problem while denoising plays a relatively minor role under small sample size.*

4.3 Color Image

In this part, we implement (robust) color image inpainting via solving the proposed minimization problem. We first illustrate the advantage of quaternion-based method over two real counterparts, i.e., the monochromatic method that completes three channels separately, the concatenation method that copes with the unfolding matrix $[R \ G \ B] \in \mathbb{R}^{d_1 \times 3d_2}$. See [25] for theories of the real (robust) completion method.



Figure 7: The original image "House" is the single image in the first column. The second column shows the observed image with sample size $n = \beta d_1 d_2$. The third, fourth, fifth column show the result of applying quaternion-based method, monochromatic method, concatenation method (resp.) to inpaint the observed image in the same row.

Under clean model (3.1), we conduct a fair comparison of three methods on two 256×256 color images "House" and "Jelly beans" from USC-SIPI image database (available online), the results are showed in Figure 7, Figure 8. Judging from PSNR the quaternion-based method outperforms other two real methods, since quaternion-based method possesses three channel as a whole and make full use of the RGB correlations. Besides, it is worthy to mention that some problems occur in monochromatic method under corrupted model (3.2): Firstly, there are three λ to tune, which is tiresome and may probably result in unbalance of three channels; Secondly, it cannot adjust to the cross-channel noise pattern since three channels are completely separated. By contrast, the noise correction strategy proposed in this work can be directly extended to the concatenation method. For more numerical examples or comparison of different types of method (e.g., tensor-based inpainting), please refer to [24].

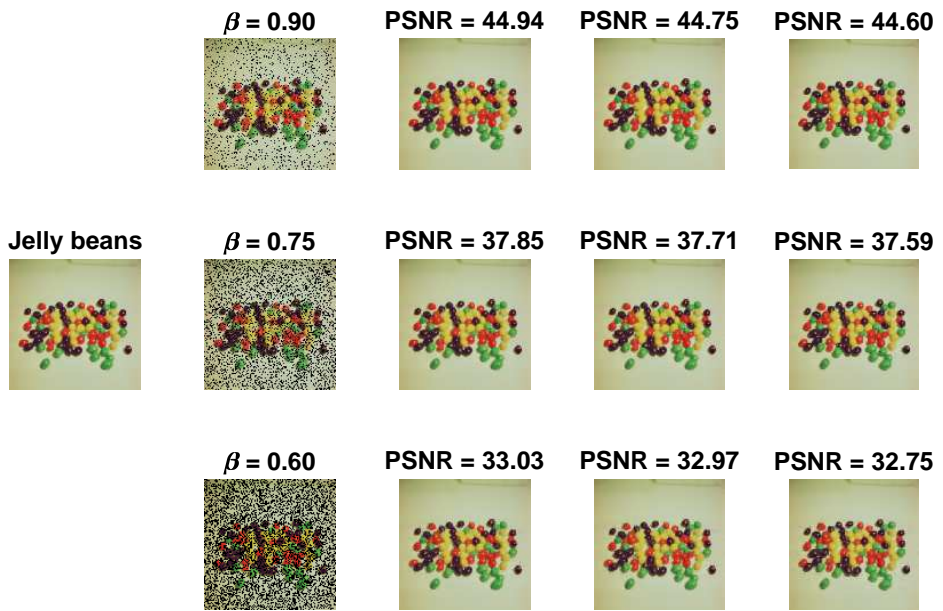


Figure 8: The original image "Jelly beans" is the single image in the first column. The second column shows the observed image with sample size $n = \beta d_1 d_2$. The third, fourth, fifth column show the result of applying quaternion-based method, monochromatic method, concatenation method (resp.) to inpaint the observed image in the same row.

Finally we provide several numerical examples to illustrate the advantage of our strategy (3.22) and (3.24) when unbalanced, correlated noise occurs. All the color images used are of size 128×128 , and can be accessed in the Linnaeus 5 dataset. In Figure 9, the red channel of the image suffers from much higher noise than other two channels. To rebalance the noise level and the data fidelity, we apply the weighted loss $\mathbf{W}(\gamma)$ given by (3.22), and search for γ over $\mathcal{G} = [0, 0.1, 0.2, 0.3, 0.4, 0.5, 0.6, 0.7, 0.8, 0.9, 1.0]$. A parallel experiment for noise correlation removal is showed in Figure 10, where the noise with equal level is highly and positively correlated. In this case the proposal (3.24) reads $\mathbf{W}(\gamma) = (1 - \gamma)\mathbf{I}_3 + \gamma\mathbf{W}_c$, and we adjust γ to optimal over \mathcal{G} . Moreover, to verify that (3.24) is an effective strategy to handle noise that is not only unbalanced but also correlated, we report other two numerical examples, the Σ_c used and the results are given in Figure 11, where the weight (γ_1, γ_2) is tuned to be optimal over $\mathcal{G} \times \mathcal{G}$. In Figure 9, Figure 10, Figure 11, the PSNR of reconstruction under \mathbf{I}_3 or a properly weighted loss are provided, indicating that the noise correction strategy is effective.

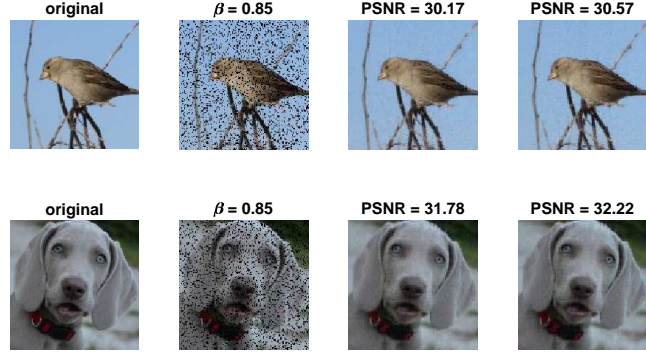


Figure 9: (Examples of noise level rebalance) The *original* images are arranged in the first column. The observed images are showed in the second column where each observations are corrupted by unbalanced noise with $\Sigma_c = \text{diag}(90, 10, 15)$. The third column shows the reconstructed image using a non-weighted loss. The last column shows the reconstructed image under $\mathbf{W}(0.7)$ in (3.22).

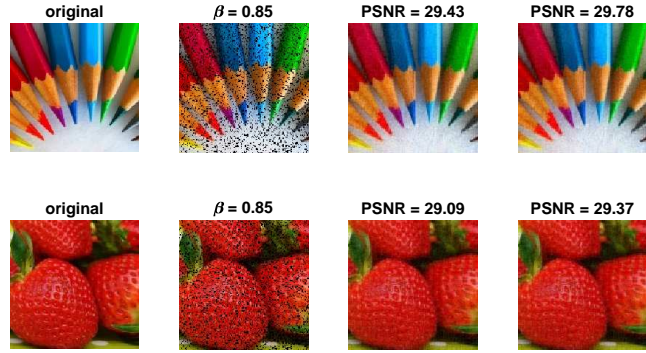


Figure 10: (Examples of noise correlation removal) The meaning of first three columns are the same as Figure 9, where $\Sigma_c = [75, 70, 65; 70, 75, 63; 65, 63, 75]$. The last column shows the reconstructed image under $\mathbf{W}(0, 0.5)$ in (3.24).

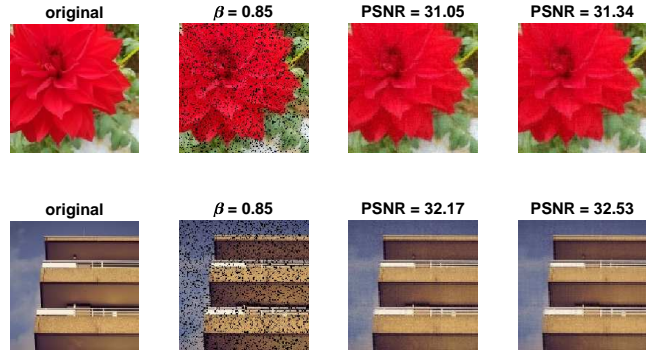


Figure 11: (Examples of combining two noise correction strategies) The meaning of first three columns are the same as Figure 9. The noise is both correlated and unbalanced: In first row, $\Sigma_c = [70, 55, 50; 55, 60, 53, 50, 53, 50]$, the last column shows the reconstructed image under $\mathbf{W}(0.1, 0.7)$ in (3.24); In second row, $\Sigma_c = [75, 70, 0; 70, 75, 0; 0, 0, 5]$, the last column shows the reconstructed image under $\mathbf{W}(0.7, 0.1)$ in (3.24).

5 Concluding Remarks

Quaternion-based method for color image inpainting was widely studied in literature. We notice that most works focus on algorithm design and convergence, or aim to propose new rank surrogate to replace nuclear norm, while the theoretical guarantee on reconstructed error remains under-developed. To our best knowledge, [24] is the only paper that presents an exact recovery guarantee, however, the stringent incoherence condition and exact low-rankness are required, which may not be satisfied by color images.

The main aim of this paper is to fill the theoretical vacancy. In this work, we formulate color image inpainting as a robust pure quaternion matrix completion problem, and obtain an error bound under much more relaxed conditions that nicely match color images. Moreover, we achieve stronger robustness than previous work [24] since all observations are corrupted, while the corrupted entries are assumed to be sufficiently sparse in their work.

To be more general, we consider a quadratic loss weighted among three channels (3.5), and the obtained error bound motivates us to handle unbalanced or highly-correlated noise via a suitable cross-channel weight. More specifically, we propose two noise correction strategies with the core spirit of rebalancing noise level, or removing noise correlation. It is interesting to note that [48] also used a diagonal weight in color image denoising, the weight therein corresponds to $\mathbf{W}(1)$ in (3.22). However, we use numerical results (Figure 5) to report that such an extreme choice may not be sensible. The underlying rationale is also provided, see our analysis on factors F_1, F_2 .

Our main results are restricted to completing a non-negative pure quaternion matrix because of the background of color image inpainting, however, all of them directly extend to general quaternion matrix completion, which is also an under-studied topic. In completion of a general quaternion matrix from corrupted observations, for example, a quadratic loss weighted by a suitable 4×4 positive definite matrix can be applied to adapt to the noise pattern, which achieves stronger robustness.

References

- [1] P. Bas, N. L. Bihan, and J. Chassery. Color image watermarking using quaternion Fourier transform. In *2003 IEEE International Conference on Acoustics, Speech, and Signal Processing, 2003. Proceedings.(ICASSP'03)*, volume 3, pages III–521. IEEE, 2003.
- [2] B. Eduardo. The theory and use of the quaternion wavelet transform. *Journal of Mathematical Imaging and Vision*, 24(1):19–35, 2006.
- [3] B. Peter and T. F. Chan. Color TV: total variation methods for restoration of vector-valued images. *IEEE transactions on image processing*, 7(3):304–309, 1998.
- [4] S. Boyd, N. Parikh, and E. Chu. Distributed optimization and statistical learning via the alternating direction method of multipliers. 2011.
- [5] T. T. Cai and A. Zhang. Sparse representation of a polytope and recovery of sparse signals and low-rank matrices. *IEEE transactions on information theory*, 60(1):122–132, 2013.

- [6] E. J. Candès and B. Rechi. Exact matrix completion via convex optimization. *Foundations of Computational mathematics*, 9(6):717–772, 2009.
- [7] E. J. Candès and T. Tao. The power of convex relaxation: Near-optimal matrix completion. *IEEE Transactions on Information Theory*, 56(5):2053–2080, 2010.
- [8] J. H. Chang and J. J. Ding. Quaternion matrix singular value decomposition and its applications for color image processing. In *Proceedings 2003 International Conference on Image Processing (Cat. No. 03CH37429)*, volume 1, pages I–805. IEEE, 2003.
- [9] B. Chen, Q. Liu, X. Sun, X. Li, and H. Shu. Removing Gaussian noise for colour images by quaternion representation and optimisation of weights in non-local means filter. *IET Image Processing*, 8(10):591–600, 2014.
- [10] B. Chen, H. Shu, G. Coatrieux, G. Chen, X. Sun, and J. L. Coatrieux. Color image analysis by quaternion-type moments. *Journal of mathematical imaging and vision*, 51(1):124–144, 2015.
- [11] B. Chen, H. Shu, H. Zhang, G. Chen, C. Toumoulin, J. Dillenseger, and L. Luo. Quaternion Zernike moments and their invariants for color image analysis and object recognition. *Signal processing*, 92(2):308–318, 2012.
- [12] G. Chen, F. Zhu, and P. A. Heng. An efficient statistical method for image noise level estimation. In *Proceedings of the IEEE International Conference on Computer Vision*, pages 477–485, 2015.
- [13] Y. Chen, X. Xiao, and Y. Zhou. Low-rank quaternion approximation for color image processing. *IEEE Transactions on Image Processing*, 29:1426–1439, 2019.
- [14] K. Dabov, A. Foi, V. Katkovnik, and K. Egiazarian. Image denoising by sparse 3-D transform-domain collaborative filtering. *IEEE Transactions on image processing*, 16(8):2080–2095, 2007.
- [15] M. Davenport and J. Romberg. An overview of low-rank matrix recovery from incomplete observations. *IEEE Journal of Selected Topics in Signal Processing*, 10(4):608–622, 2016.
- [16] T. A. Ell and S. J. Sangwine. Hypercomplex Fourier transforms of color images. *IEEE Transactions on image processing*, 16(1):22–35, 2006.
- [17] R. Foygel and N. Srebro. Concentration-based guarantees for low-rank matrix reconstruction. In *Proceedings of the 24th Annual Conference on Learning Theory*, pages 315–340. JMLR Workshop and Conference Proceedings, 2011.
- [18] D. Gabay and B. Mercier. A dual algorithm for the solution of nonlinear variational problems via finite element approximation. *Computers & mathematics with applications*, 2(1):17–40, 1976.
- [19] S. Gai, G. Yang, M. Wan, and L. Wang. Denoising color images by reduced quaternion matrix singular value decomposition. *Multidimensional Systems and Signal Processing*, 26(1):307–320, 2015.

- [20] N. Gillis and F. Glineur. Low-rank matrix approximation with weights or missing data is NP-hard. *SIAM Journal on Matrix Analysis and Applications*, 32(4):1149–1165, 2011.
- [21] X. Han, J. Wu, L. Yan, L. Senhadji, and H. Shu. Color image recovery via quaternion matrix completion. In *2013 6th International Congress on Image and Signal Processing (CISP)*, volume 1, pages 358–362. IEEE, 2013.
- [22] C. Huang, M. K. Ng, T. Wu, and T. Zeng. Quaternion-based Dictionary Learning and Saturation-Value Total Variation Regularization for Color Image Restoration. *IEEE Transactions on Multimedia*, 2021.
- [23] Z. Jia, Q. Jin, M. K. Ng, and X. Zhao. Non-Local Robust Quaternion Matrix Completion for Large-Scale Color Images and Videos Inpainting. *arXiv preprint arXiv:2011.08675*, 2020.
- [24] Z. Jia, M. K. Ng, and G. Song. Robust quaternion matrix completion with applications to image inpainting. *Numerical Linear Algebra with Applications*, 26(4):e2245, 2019.
- [25] O. Klopp. Noisy low-rank matrix completion with general sampling distribution. *Bernoulli*, 20(1):282–303, 2014.
- [26] N. L. Bihan and S. J. Sangwine. Color image decomposition using quaternion singular value decomposition. In *2003 International Conference on Visual Information Engineering VIE 2003*, pages 113–116. IET, 2003.
- [27] X. Liu, M. Tanaka, and M. Okutomi. Single-image noise level estimation for blind denoising. *IEEE transactions on image processing*, 22(12):5226–5237, 2013.
- [28] J. Miao and K. I. Kou. Quaternion-based bilinear factor matrix norm minimization for color image inpainting. *IEEE Transactions on Signal Processing*, 68:5617–5631, 2020.
- [29] J. Miao and K. I. Kou. Color image recovery using low-rank quaternion matrix completion algorithm. *IEEE Transactions on Image Processing*, 2022.
- [30] J. Miao, K. I. Kou, and W. Liu. Low-rank quaternion tensor completion for recovering color videos and images. *Pattern Recognition*, 107:107505, 2020.
- [31] T. Mizoguchi and I. Yamada. Hypercomplex low rank matrix completion with non-negative constraints via convex optimization. In *ICASSP 2019-2019 IEEE International Conference on Acoustics, Speech and Signal Processing (ICASSP)*, pages 8538–8542. IEEE, 2019.
- [32] S. Nam, Y. Hwang, Y. Matsushita, and S. J. Kim. A holistic approach to cross-channel image noise modeling and its application to image denoising. In *Proceedings of the IEEE conference on computer vision and pattern recognition*, pages 1683–1691, 2016.
- [33] S. Negahban and M. J. Wainwright. Restricted strong convexity and weighted matrix completion: Optimal bounds with noise. *The Journal of Machine Learning Research*, 13(1):1665–1697, 2012.

- [34] S. Negahban, P. Ravikumar, M. J. Wainwright, and B. Yu. A unified framework for high-dimensional analysis of M -estimators with decomposable regularizers. *Statistical science*, 27(4):538–557, 2012.
- [35] T. Parcollet, M. Morchid, and G. Linares. Quaternion convolutional neural networks for heterogeneous image processing. In *ICASSP 2019-2019 IEEE International Conference on Acoustics, Speech and Signal Processing (ICASSP)*, pages 8514–8518. IEEE, 2019.
- [36] S. C. Pei and C. M. Cheng. A novel block truncation coding of color images using a quaternion-moment-preserving principle. *IEEE Transactions on Communications*, 45(5):583–595, 1997.
- [37] S. C. Pei and C. M. Cheng. Color image processing by using binary quaternion-moment-preserving thresholding technique. *IEEE Transactions on Image Processing*, 8(5):614–628, 1999.
- [38] B. Rechi. A Simpler Approach to Matrix Completion. *Journal of Machine Learning Research*, 12(12), 2011.
- [39] S. J. Sangwine. Fourier transforms of colour images using quaternion or hypercomplex numbers. *Electronics letters*, 32(21):1979–1980, 1996.
- [40] L. Shi and B. Funt. Quaternion color texture segmentation. *Computer Vision and image understanding*, 107(1-2):88–96, 2007.
- [41] G. Song, W. Ding, and M. K. Ng. Low Rank Pure Quaternion Approximation for Pure Quaternion Matrices. *SIAM Journal on Matrix Analysis and Applications*, 42(1):58–82, 2021.
- [42] Ö. N. Subakan and B. C. Vemuri. A quaternion framework for color image smoothing and segmentation. *International Journal of Computer Vision*, 91(3):233–250, 2011.
- [43] Y. Sun, S. Chen, and B. Yin. Color face recognition based on quaternion matrix representation. *Pattern Recognition Letters*, 32(4):597–605, 2011.
- [44] J. A. Tropp. User-friendly tail bounds for sums of random matrices. *Foundations of computational mathematics*, 12(4):389–434, 2012.
- [45] J. A. Tropp. An introduction to matrix concentration inequalities. *arXiv preprint arXiv:1501.01571*, 2015.
- [46] S. A. van de Geer. *Estimation and testing under sparsity*. Springer, 2016.
- [47] M. J. Wainwright. High-dimensional statistics: A non-asymptotic viewpoint. volume 48. Cambridge University Press, 2019.
- [48] J. Xu, L. Zhang, D. Zhang, and X. Feng. Multi-channel weighted nuclear norm minimization for real color image denoising. In *Proceedings of the IEEE international conference on computer vision*, pages 1096–1104, 2017.

[49] Y. Xu, Y. Yu, H. Xu, H. Zhang, and T. Nguyen. Vector sparse representation of color image using quaternion matrix analysis. *IEEE Transactions on image processing*, 24(4):1315–1329, 2015.

[50] L. Yang, K. I. Kou, and J. Miao. Weighted Truncated Nuclear Norm Regularization for Low-Rank Quaternion Matrix Completion. *arXiv preprint arXiv:2101.02443*, 2021.

[51] L. Yang, J. Miao, and K. I. Kou. Low Rank Quaternion Matrix Recovery via Logarithmic Approximation. *arXiv preprint arXiv:2107.01380*, 2021.

[52] M. Yu, Y. Xu, and P. Sun. Single color image super-resolution using quaternion-based sparse representation. In *2014 IEEE International Conference on Acoustics, Speech and Signal Processing (ICASSP)*, pages 5804–5808. IEEE, 2014.

[53] Y. Yu, Y. Zhang, and S. Yuan. Quaternion-based weighted nuclear norm minimization for color image denoising. *Neurocomputing*, 332:283–297, 2019.

[54] F. Zhang. Quaternions and matrices of quaternions. *Linear algebra and its applications*, 251:21–57, 1997.

[55] X. Zhu, Y. Xu, H. Xu, and C. Chen. Quaternion convolutional neural networks. In *Proceedings of the European Conference on Computer Vision (ECCV)*, pages 631–647, 2018.

A Proofs of Technical Tools

Proof of Lemma 1. Assume $\text{rank}(\mathbf{A}) = r \leq \min\{M, N\}$, then \mathbf{A} has r positive singular values $\sigma_1(\mathbf{A}) \geq \sigma_2(\mathbf{A}) \geq \dots \geq \sigma_r(\mathbf{A})$. Then we have

$$\|\mathbf{A}\|_{\text{nu}} = \sum_{i \in [r]} \sigma_i(\mathbf{A}) \leq \sqrt{(\sum_{i \in [r]} 1^2)(\sum_{i \in [r]} \sigma_i(\mathbf{A})^2)} \leq \sqrt{r} \|\mathbf{A}\|_{\text{F}},$$

where we use Cauchy inequality. \square

Proof of Lemma 2. I. We first show that we can only consider square matrices with no loss of generality. If $M < N$, we consider

$$\tilde{\mathbf{A}} = \begin{bmatrix} \mathbf{A} \\ \mathbf{0} \end{bmatrix}, \quad \tilde{\mathbf{B}} = \begin{bmatrix} \mathbf{B} \\ \mathbf{0} \end{bmatrix} \in \mathbb{Q}^{N \times N};$$

If $M > N$ we consider $\tilde{\mathbf{A}} = [\mathbf{A} \ \mathbf{0}]$, $\tilde{\mathbf{B}} = [\mathbf{B} \ \mathbf{0}] \in \mathbb{Q}^{M \times M}$. It can be easily seen that both transforms preserve inner product, nuclear norm and operator norm.

II. Assume $\mathbf{A}, \mathbf{B} \in \mathbb{Q}^{M \times M}$, and $\mathbf{B} = \mathbf{U}\Sigma\mathbf{V}^*$ is the QSVD of \mathbf{B} , where $\mathbf{U}, \mathbf{V} \in \mathbb{Q}^{M \times M}$ are unitary, and $\Sigma = \text{diag}(\sigma_1, \dots, \sigma_M) \in \mathbb{R}^{M \times M}$. Then

$$\langle \mathbf{A}, \mathbf{B} \rangle = \text{Tr}(\mathbf{A}^* \mathbf{B}) = \text{Tr}(\mathbf{A}^* \mathbf{U} \Sigma \mathbf{V}^*) = \text{Tr}(\mathbf{C} \Sigma \mathbf{V}^*),$$

where we let $\mathbf{A}^* \mathbf{U} = \mathbf{C} = [\mathbf{c}_{ij}] \in \mathbb{Q}^{M \times M}$. Let $\mathbf{U} = [u_1, \dots, u_M]$, then the i -th ($i \in [M]$) column of \mathbf{C} is $\mathbf{A}^* u_i$, so the ℓ_2 norm of columns of \mathbf{C} are bounded by $\|\mathbf{A}^* u_i\|_2 \leq \|\mathbf{A}^*\|_{\text{op}} \|u_i\|_2 = \|\mathbf{A}\|_{\text{op}}$. Further let $\mathbf{V}^* = [\mathbf{v}_{ij}]$, then we compute element-wisely:

$$\begin{aligned}
|\text{Tr}(\mathbf{C} \Sigma \mathbf{V}^*)| &= \left| \sum_{i \in [M]} \sum_{j \in [M]} \mathbf{c}_{ij} \sigma_j \mathbf{v}_{ji} \right| \\
&= \left| \sum_j \left(\sum_i \mathbf{c}_{ij} \mathbf{v}_{ji} \right) \sigma_j \right| \\
&\leq \sum_j \left| \sum_i \mathbf{c}_{ij} \mathbf{v}_{ji} \right| \sigma_j \\
&\leq \sum_j \left[\|\mathbf{A}^* u_j\|_2^2 \left(\sum_i |\mathbf{v}_{ji}|^2 \right) \right]^{1/2} \sigma_j \\
&\leq \|\mathbf{A}\|_{\text{op}} \sum_j \sigma_j \\
&= \|\mathbf{A}\|_{\text{op}} \|\mathbf{B}\|_{\text{nu}},
\end{aligned}$$

hence the result follows. \square

Proof of Lemma 3. We only consider square matrix $\mathbf{A} \in \mathbb{Q}^{M \times M}$ for the same reason as Lemma 2. Let $\mathbf{B} = \mathbf{A}_0 + \mathbf{A}_1 \mathbf{i}$, $\mathbf{C} = \mathbf{A}_2 + \mathbf{A}_3 \mathbf{i} \in \mathbb{C}^{M \times M}$, then $\mathbf{A} = \mathbf{B} + \mathbf{C} \mathbf{j}$. Denote the set of $M \times M$ quaternion unitary matrices, complex unitary matrices, (real) orthogonal matrices by $\mathcal{U}_{\mathbb{Q}}$, $\mathcal{U}_{\mathbb{C}}$, and $\mathcal{U}_{\mathbb{R}}$ respectively, evidently, $\mathcal{U}_{\mathbb{R}} \subset \mathcal{U}_{\mathbb{C}} \subset \mathcal{U}_{\mathbb{Q}}$. By Theorem 5 in [51] we have

$$\|\mathbf{A}\|_{\text{nu}} = \sup_{\mathbf{U}, \mathbf{V} \in \mathcal{U}_{\mathbb{Q}}} |\text{Tr}(\mathbf{U} \mathbf{A} \mathbf{V}^*)|,$$

which delivers that

$$\begin{aligned}
\|\mathbf{A}\|_{\text{nu}} &\geq \sup_{\mathbf{U}, \mathbf{V} \in \mathcal{U}_{\mathbb{C}}} |\text{Tr}(\mathbf{U} \mathbf{A} \mathbf{V}^*)| \\
&= \sup_{\mathbf{U}, \mathbf{V} \in \mathcal{U}_{\mathbb{C}}} |\text{Tr}(\mathbf{U} [\mathbf{B} + \mathbf{C} \mathbf{j}] \mathbf{V}^*)| \\
&= \sup_{\mathbf{U}, \mathbf{V} \in \mathcal{U}_{\mathbb{C}}} |\text{Tr}(\mathbf{U} \mathbf{B} \mathbf{V}^*) + \text{Tr}(\mathbf{U} \mathbf{C} \mathbf{V}^T) \mathbf{j}| \\
&\geq \sup_{\mathbf{U}, \mathbf{V} \in \mathcal{U}_{\mathbb{C}}} |\text{Tr}(\mathbf{U} \mathbf{B} \mathbf{V}^*)| \\
&= \|\mathbf{B}\|_{\text{nu}},
\end{aligned}$$

by complex SVD of \mathbf{B} it is not hard to show the last equality. We can further proceed it by

$$\begin{aligned}
\|\mathbf{B}\|_{\text{nu}} &= \sup_{\mathbf{U}, \mathbf{V} \in \mathcal{U}_{\mathbb{C}}} |\text{Tr}(\mathbf{U} \mathbf{B} \mathbf{V}^*)| \\
&\geq \sup_{\mathbf{U}, \mathbf{V} \in \mathcal{U}_{\mathbb{R}}} |\text{Tr}(\mathbf{U} [\mathbf{A}_0 + \mathbf{A}_1 \mathbf{i}] \mathbf{V}^*)| \\
&= \sup_{\mathbf{U}, \mathbf{V} \in \mathcal{U}_{\mathbb{R}}} |\text{Tr}(\mathbf{U} \mathbf{A}_0 \mathbf{V}^*) + \text{Tr}(\mathbf{U} \mathbf{A}_1 \mathbf{V}^*) \mathbf{i}| \\
&\geq \sup_{\mathbf{U}, \mathbf{V} \in \mathcal{U}_{\mathbb{R}}} |\text{Tr}(\mathbf{U} \mathbf{A}_0 \mathbf{V}^*)| \\
&= \|\mathbf{A}_0\|_{\text{nu}},
\end{aligned}$$

by real SVD of \mathbf{A}_0 we can verify the last equality. \square

Proof of Corollary 1. Let $\boldsymbol{\nu}$ be the unit quaternion $\nu_0 - \nu_1 \mathbf{i} - \nu_2 \mathbf{j} - \nu_3 \mathbf{k}$, we consider $\boldsymbol{\nu} \mathbf{A}$, then we have $\|\boldsymbol{\nu} \mathbf{A}\|_{\text{nu}} = \|\mathbf{A}\|_{\text{nu}}$. Evidently, we have

$$[\boldsymbol{\nu} \mathbf{A}]_1 = \nu_0 \mathbf{A}_0 + \nu_1 \mathbf{A}_1 + \nu_2 \mathbf{A}_2 + \nu_3 \mathbf{A}_3,$$

then the result follows by using Lemma 3. \square

Proof of Lemma 4. We consider the complex adjoint $\{[\mathbf{S}_1]_{\mathbb{C}}, \dots, [\mathbf{S}_n]_{\mathbb{C}}\} \subset \mathbb{C}^{2M \times 2M}$, which are independent Hermitian random matrices with zero mean. Note that $[\cdot]_{\mathbb{C}}$ preserves the operator norm, expectation, and multiplication, so for any integer $p \geq 2$ we have

$$\frac{1}{2} p! R^{p-2} \sigma^2 \geq \|\mathbb{E} \mathbf{S}_k^p\|_{\text{op}} = \|\mathbb{E} [\mathbf{S}_k^p]_{\mathbb{C}}\|_{\text{op}} = \|\mathbb{E} [\mathbf{S}_k^p]_{\mathbb{C}}\|_{\text{op}} = \|\mathbb{E} [\mathbf{S}_k]_{\mathbb{C}}^p\|_{\text{op}}.$$

Then by using Theorem 6.2 in [44], for any $t > 0$ we have

$$\begin{aligned} & \mathbb{P} \left[\left\| \frac{1}{n} \sum_{k=1}^n \mathbf{S}_k \right\|_{\text{op}} \geq t \right] \\ &= \mathbb{P} \left[\left\| \sum_{k=1}^n [\mathbf{S}_k]_{\mathbb{C}} \right\|_{\text{op}} \geq nt \right] \\ &\leq \mathbb{P} \left[\lambda_{\max} \left(\sum_{k=1}^n [\mathbf{S}_k]_{\mathbb{C}} \right) \geq nt \right] + \mathbb{P} \left[\lambda_{\max} \left(\sum_{k=1}^n [-\mathbf{S}_k]_{\mathbb{C}} \right) \geq nt \right] \\ &\leq 2M \exp \left(-\frac{n^2 t^2}{2(n\sigma^2 + Rnt)} \right) + 2M \exp \left(-\frac{n^2 t^2}{2(n\sigma^2 + Rnt)} \right) \\ &\leq 4M \exp \left(-\frac{nt^2}{2(\sigma^2 + Rt)} \right), \end{aligned}$$

which finishes the proof. \square

B Proofs of Main Results

B.1 Error Bound

Proof of Lemma 5. I. We first decompose the complementary event into countably infinite events. State the complementary event as

$$\mathcal{B} = \{\exists \boldsymbol{\Theta}_0 \in \mathcal{C}(\psi), \text{ s.t. } \mathcal{F}_{\mathcal{X}}(\boldsymbol{\Theta}_0) \leq \frac{\kappa}{d_1 d_2} \|\boldsymbol{\Theta}_0\|_{\text{w,F}}^2 - T_0\},$$

note that $\mathbb{E} \mathcal{F}_{\mathcal{X}}(\boldsymbol{\Theta}) = \|\boldsymbol{\Theta}\|_{\text{w,F}}^2 / (d_1 d_2)$, so \mathcal{B} implies

$$|\mathcal{F}_{\mathcal{X}}(\boldsymbol{\Theta}_0) - \mathbb{E} \mathcal{F}_{\mathcal{X}}(\boldsymbol{\Theta}_0)| \geq \left(\frac{1 - \kappa}{d_1 d_2} \right) \|\boldsymbol{\Theta}_0\|_{\text{w,F}}^2 + T_0. \quad (\text{B.1})$$

By (3.9) we know

$$\|\boldsymbol{\Theta}_0\|_{\text{w,F}}^2 \geq D_0 =: \alpha^2 d_1 d_2 \sqrt{\frac{\psi_3 \log(d_1 + d_2)}{n}},$$

hence by a fixed $\zeta > 1$ (which will be specified later) there exists positive integer l such that $\|\Theta_0\|_{w,F}^2 \in [\zeta^{l-1}D_0, \zeta^l D_0]$, hence

$$\Theta_0 \in \mathcal{C}(\psi, l) := \mathcal{C}(\psi) \cap \{\Theta : \|\Theta\|_{w,F}^2 \in [\zeta^{l-1}D_0, \zeta^l D_0]\}. \quad (\text{B.2})$$

We define

$$\mathcal{Z}_{\mathcal{X}}(l) = \sup_{\Theta \in \mathcal{C}(\psi, l)} |\mathcal{F}_{\mathcal{X}}(\Theta) - \mathbb{E}\mathcal{F}_{\mathcal{X}}(\Theta)|,$$

then by combining (B.1), (B.2) we know the event defined by

$$\mathcal{B}_l := \left\{ \mathcal{Z}_{\mathcal{X}}(l) \geq \left(\frac{1-\kappa}{d_1 d_2} \right) \zeta^{l-1} D_0 + T_0 \right\} \quad (\text{B.3})$$

holds. Therefore, we have

$$\mathbb{P}(\mathcal{B}) \leq \sum_{l=1}^{\infty} \mathbb{P}(\mathcal{B}_l). \quad (\text{B.4})$$

II. It suffices to bound $\mathbb{P}(\mathcal{B}_l)$ for positive integer l . We first bound the deviation $|\mathcal{Z}_{\mathcal{X}}(l) - \mathbb{E}\mathcal{Z}_{\mathcal{X}}(l)|$. Let $\widetilde{\mathcal{X}} = \{\widetilde{\mathbf{X}_1}, \mathbf{X}_2, \dots, \mathbf{X}_n\}$, i.e., only the first component may vary from \mathcal{X} , then for any positive integer l we have

$$\begin{aligned} & \sup_{\mathcal{X}, \widetilde{\mathcal{X}}} |\mathcal{Z}_{\mathcal{X}}(l) - \mathcal{Z}_{\widetilde{\mathcal{X}}}(l)| \\ &= \sup_{\mathcal{X}, \widetilde{\mathcal{X}}} \left| \sup_{\Theta \in \mathcal{C}(\psi, l)} |\mathcal{F}_{\mathcal{X}}(\Theta) - \mathbb{E}\mathcal{F}_{\mathcal{X}}(\Theta)| - \sup_{\Theta \in \mathcal{C}(\psi, l)} |\mathcal{F}_{\widetilde{\mathcal{X}}}(\Theta) - \mathbb{E}\mathcal{F}_{\widetilde{\mathcal{X}}}(\Theta)| \right| \\ &\leq \sup_{\mathcal{X}, \widetilde{\mathcal{X}}} \left| \sup_{\Theta \in \mathcal{C}(\psi, l)} |\mathcal{F}_{\mathcal{X}}(\Theta) - \mathcal{F}_{\widetilde{\mathcal{X}}}(\Theta)| \right| \\ &= \sup_{\mathbf{X}_1, \widetilde{\mathbf{X}}_1} \sup_{\Theta \in \mathcal{C}(\psi, l)} \frac{1}{n} \left| |\langle \mathbf{X}_1, \Theta \rangle|_w^2 - |\langle \widetilde{\mathbf{X}}_1, \Theta \rangle|_w^2 \right| \\ &\leq \frac{\psi_1^2 \alpha^2}{n}, \end{aligned}$$

where we use $\|\Theta\|_{w,\infty} \leq \psi_1 \alpha$ in the last line. Since n components in \mathcal{X} are symmetrical, by bounded difference inequality (e.g., Corollary 2.21, [47]), for any $t > 0$ we have

$$\mathbb{P}[\mathcal{Z}_{\mathcal{X}}(l) - \mathbb{E}\mathcal{Z}_{\mathcal{X}}(l) \geq t] \leq \exp\left(-\frac{2nt^2}{\psi_1^4 \alpha^4}\right). \quad (\text{B.5})$$

It remains to bound $\mathbb{E}\mathcal{Z}_{\mathcal{X}}(l)$. Let $\mathcal{E} = (\varepsilon_1, \dots, \varepsilon_n)$ be i.i.d. Rademacher random variables ($\mathbb{P}[\varepsilon_k = 1] = \mathbb{P}[\varepsilon_k = -1] = 1/2$), then by symmetrization of expectations (e.g., Theorem 16.1, [46]), we have

$$\begin{aligned} \mathbb{E}\mathcal{Z}_{\mathcal{X}}(l) &= \mathbb{E} \sup_{\Theta \in \mathcal{C}(\psi, l)} |\mathcal{F}_{\mathcal{X}}(\Theta) - \mathbb{E}\mathcal{F}_{\mathcal{X}}(\Theta)| \\ &= \mathbb{E} \sup_{\Theta \in \mathcal{C}(\psi, l)} \left| \frac{1}{n} \sum_{k=1}^n \left\{ |\langle \mathbf{X}_k, \Theta \rangle|_w^2 - \mathbb{E}|\langle \mathbf{X}_k, \Theta \rangle|_w^2 \right\} \right| \\ &\leq 2\mathbb{E} \sup_{\Theta \in \mathcal{C}(\psi, l)} \left| \frac{1}{n} \sum_{k=1}^n \varepsilon_k |\langle \mathbf{X}_k, \Theta \rangle|_w^2 \right| \\ &= 2\mathbb{E}_{\mathcal{X}} \mathbb{E}_{\mathcal{E}} \sup_{\Theta \in \mathcal{C}(\psi, l)} \left| \frac{1}{n} \sum_{k=1}^n \varepsilon_k |\langle \mathbf{X}_k, \sqrt{\mathbf{W}}\Theta \rangle|^2 \right|, \end{aligned} \quad (\text{B.6})$$

where $\mathbb{E}_{\mathcal{X}}, \mathbb{E}_{\mathcal{E}}$ denote taking expectation of the random variables in subscript. Moreover, by dividing three parts, applying Talagrand's inequality (e.g., Theorem 16.2, [46]) we have

$$\begin{aligned}
& \mathbb{E}_{\mathcal{E}} \sup_{\Theta \in \mathcal{C}(\psi, l)} \left| \frac{1}{n} \sum_{k=1}^n \varepsilon_k \langle \mathbf{X}_k, \sqrt{\mathbf{W}} \Theta \rangle \right|^2 \\
& \leq (2\psi_1 \alpha)^2 \sum_{\vartheta \in \{\mathbf{i}, \mathbf{j}, \mathbf{k}\}} \mathbb{E}_{\mathcal{E}} \sup_{\Theta \in \mathcal{C}(\psi, l)} \left| \frac{1}{n} \sum_{k=1}^n \varepsilon_k \langle \mathbf{X}_k, [\sqrt{\mathbf{W}} \Theta]_{\vartheta} (2\psi_1 \alpha)^{-1} \rangle^2 \right| \\
& \leq 4\psi_1 \alpha \sum_{\vartheta \in \{\mathbf{i}, \mathbf{j}, \mathbf{k}\}} \mathbb{E}_{\mathcal{E}} \sup_{\Theta \in \mathcal{C}(\psi, l)} \left| \langle \frac{1}{n} \sum_{k=1}^n \varepsilon_k \mathbf{X}_k, [\sqrt{\mathbf{W}} \Theta]_{\vartheta} \rangle \right|.
\end{aligned} \tag{B.7}$$

By plugging (B.7) in (B.6) and using Corollary 1, it yields that

$$\begin{aligned}
\mathbb{E} \mathcal{Z}_{\mathcal{X}}(l) & \leq 8\psi_1 \alpha \sum_{\vartheta \in \{\mathbf{i}, \mathbf{j}, \mathbf{k}\}} \left\{ \mathbb{E} \left\| \frac{1}{n} \sum_{k=1}^n \varepsilon_k \mathbf{X}_k \right\|_{\text{op}} \right\} \sup_{\Theta \in \mathcal{C}(\psi, l)} \left\| [\sqrt{\mathbf{W}} \Theta]_{\vartheta} \right\|_{\text{nu}} \\
& \leq 24\psi_1 \alpha \left\{ \mathbb{E} \left\| \frac{1}{n} \sum_{k=1}^n \varepsilon_k \mathbf{X}_k \right\|_{\text{op}} \right\} \|\sqrt{\mathbf{W}}\|_{2, \infty} \sup_{\Theta \in \mathcal{C}(\psi, l)} \|\Theta\|_{\text{nu}} \\
& \leq 24\psi_1 \psi_2 \rho^{\frac{1}{2-q}} \alpha \left\{ \mathbb{E} \left\| \frac{1}{n} \sum_{k=1}^n \varepsilon_k \mathbf{X}_k \right\|_{\text{op}} \right\} \|\sqrt{\mathbf{W}}\|_{2, \infty} \sup_{\Theta \in \mathcal{C}(\psi, l)} \|\Theta\|_{\text{F}}^{\frac{2-2q}{2-q}},
\end{aligned} \tag{B.8}$$

while clearly we have $\|\sqrt{\mathbf{W}}\|_{2, \infty} = \sqrt{\|\mathbf{W}\|_{\infty}}$. By Matrix Bernstein (Theorem 6.1.1, [45]) it is not hard to show (assume $[\min\{d_1, d_2\} \log(d_1 + d_2)]/n \leq 1/16$)

$$\mathbb{E} \left\| \frac{1}{n} \sum_{k=1}^n \varepsilon_k \mathbf{X}_k \right\|_{\text{op}} \leq \frac{3}{2} (d_1 d_2)^{-\frac{1}{2}} \sqrt{\frac{\max\{d_1, d_2\} \log(d_1 + d_2)}{n}}. \tag{B.9}$$

By (B.2) we know for any $\Theta \in \mathcal{C}(\psi, l)$ it holds that

$$\zeta^l D_0 \geq \|\Theta\|_{\text{w, F}}^2 \geq \lambda_{\min}(\mathbf{W}) \|\Theta\|_{\text{F}}^2 \tag{B.10}$$

Plug (B.9), (B.10) in (B.8), some algebra yields

$$\mathbb{E} \mathcal{Z}_{\mathcal{X}}(l) \leq \left\{ (2-q) T_0 \right\}^{\frac{1}{2-q}} \left\{ \frac{\zeta^l D_0}{d_1 d_2} \right\}^{\frac{1-q}{2-q}} \leq \frac{1-q}{2-q} \frac{\zeta^l D_0}{d_1 d_2} + T_0 \tag{B.11}$$

By combining with (B.3), (B.5), we have

$$\begin{aligned}
\mathbb{P}(\mathcal{B}_l) & \leq \mathbb{P} \left[\mathcal{Z}_{\mathcal{X}}(l) - \mathbb{E} \mathcal{Z}_{\mathcal{X}}(l) \geq \left(\frac{1-\kappa}{\zeta} - \frac{1-q}{2-q} \right) \frac{\zeta^l D_0}{d_1 d_2} \right] \\
& \leq \exp \left(-\frac{2n\kappa_1^2 \zeta^{2l} D_0^2}{\psi_1^4 \alpha^4 (d_1 d_2)^2} \right),
\end{aligned} \tag{B.12}$$

where we let $\kappa_1 = \frac{1-\kappa}{\zeta} - \frac{1-q}{2-q}$, which is in $(0, 1)$ by letting κ close to 0, ζ close to 1. We then

take the union bound, plug in D_0 , and use $\zeta^{2l} > 2l \log \zeta$

$$\begin{aligned} \mathbb{P}(\mathcal{B}) &\leq \sum_{l=1}^{\infty} \mathbb{P}(\mathcal{B}_l) \\ &\leq \sum_{l=1}^{\infty} (d_1 + d_2)^{-\frac{4\psi_3\kappa_1^2 \log \zeta}{\psi_1^4} l} \\ &\leq 2(d_1 + d_2)^{-3/4}, \end{aligned} \tag{B.13}$$

the last inequality holds if we let

$$\psi_3 \geq \frac{3\psi_1^4}{16\kappa_1^2 \log \zeta}.$$

□

Proof of Lemma 6. (1) I. We first introduce a pair of subspaces $(\mathcal{M}, \overline{\mathcal{M}})$ and build some useful inequalities. Write the QSVD of $\tilde{\Theta}$ as

$$\mathbf{U}\Sigma\mathbf{V}^* = [\mathbf{U}_1 \ \mathbf{U}_2] \begin{bmatrix} \Sigma_{11} & \mathbf{0} \\ \mathbf{0} & \Sigma_{22} \end{bmatrix} \begin{bmatrix} \mathbf{V}_1^* \\ \mathbf{V}_2^* \end{bmatrix}, \tag{B.14}$$

where $\mathbf{U}_1 \in \mathbb{Q}^{d_1 \times z}$, $\mathbf{U}_2 \in \mathbb{Q}^{d_1 \times (d_1-z)}$ are partition of left singular vectors, $\mathbf{V}_1 \in \mathbb{Q}^{d_2 \times z}$, $\mathbf{V}_2 \in \mathbb{Q}^{d_2 \times (d_2-z)}$ are partition of right singular vectors, the diagonal of $\Sigma_{11} \in \mathbb{R}^{z \times z}$ contains the z largest singular values, the remaining $\min\{d_1, d_2\} - z$ singular values are arranged in Σ_{22} , here the integer $z \in \{0, 1, \dots, \min\{d_1, d_2\}\}$ will be selected later. Corresponding to a specific z we define the subspace $\mathcal{M}, \overline{\mathcal{M}} \in \mathbb{Q}^{d_1 \times d_2}$ by

$$\mathcal{M} = \{\mathbf{U}_1 \mathbf{A}_1 \mathbf{V}_1^* : \mathbf{A}_1 \in \mathbb{Q}^{z \times z}\},$$

$$\overline{\mathcal{M}} = \left\{ [\mathbf{U}_1 \ \mathbf{U}_2] \begin{bmatrix} \mathbf{A}_1 & \mathbf{A}_2 \\ \mathbf{A}_3 & \mathbf{0} \end{bmatrix} \begin{bmatrix} \mathbf{V}_1^* \\ \mathbf{V}_2^* \end{bmatrix} : \mathbf{A}_1 \in \mathbb{Q}^{z \times z}, \mathbf{A}_2 \in \mathbb{Q}^{z \times (d_1-z)}, \mathbf{A}_3 \in \mathbb{Q}^{(d_1-z) \times z} \right\}.$$

We use $\mathcal{P}_{\mathcal{M}}, \mathcal{P}_{\overline{\mathcal{M}}}$ to denote the projection onto $\mathcal{M}, \overline{\mathcal{M}}$ respectively. Consider any $\Delta \in \mathbb{Q}^{d_1 \times d_2}$

$$\Delta = [\mathbf{U}_1 \ \mathbf{U}_2] \begin{bmatrix} \Delta_{11} & \Delta_{12} \\ \Delta_{21} & \Delta_{22} \end{bmatrix} \begin{bmatrix} \mathbf{V}_1^* \\ \mathbf{V}_2^* \end{bmatrix},$$

$\mathcal{P}_{\mathcal{M}}$ and $\mathcal{P}_{\overline{\mathcal{M}}}$ can be given explicitly as

$$\mathcal{P}_{\mathcal{M}}\Delta = \mathbf{U}_1 \Delta_{11} \mathbf{V}_1^*; \quad \mathcal{P}_{\overline{\mathcal{M}}}\Delta = [\mathbf{U}_1 \ \mathbf{U}_2] \begin{bmatrix} \Delta_{11} & \Delta_{12} \\ \Delta_{21} & \Delta_{22} \end{bmatrix} \begin{bmatrix} \mathbf{V}_1^* \\ \mathbf{V}_2^* \end{bmatrix}.$$

Besides, we let $\mathcal{P}_{\mathcal{M}^\perp}\Delta = \Delta - \mathcal{P}_{\mathcal{M}}\Delta$, $\mathcal{P}_{\overline{\mathcal{M}}^\perp}\Delta = \Delta - \mathcal{P}_{\overline{\mathcal{M}}}\Delta$. Note that nuclear norm is decomposable [33] with respect to $(\mathcal{M}, \overline{\mathcal{M}})$ in the sense that

$$\|\mathcal{P}_{\mathcal{M}}\Delta_1 + \mathcal{P}_{\overline{\mathcal{M}}^\perp}\Delta_2\|_{\text{nu}} = \|\mathcal{P}_{\mathcal{M}}\Delta_1\|_{\text{nu}} + \|\mathcal{P}_{\overline{\mathcal{M}}^\perp}\Delta_2\|_{\text{nu}}, \quad \forall \Delta_1, \Delta_2 \in \mathbb{Q}^{d_1 \times d_2}. \tag{B.15}$$

Let $\sigma_1(\tilde{\Theta}) \geq \dots \geq \sigma_{\min\{d_1, d_2\}}(\tilde{\Theta})$ be the singular values of $\tilde{\Theta}$, we specify a threshold $\tau > 0$, and then determine z by:

$$z = \max \left\{ \{0\} \cup \{i \in [\min\{d_1, d_2\}] : \sigma_i(\tilde{\Theta}) \geq \tau\} \right\}.$$

Recall the approximate low-rankness (3.8), we have

$$\rho \geq \sum_{i=1}^z \sigma_i(\tilde{\Theta})^q \geq \tau^q z \implies z \leq \rho \tau^{-q}. \quad (\text{B.16})$$

For the $\min\{d_1, d_2\} - z$ smallest singular values we have

$$\|\mathcal{P}_{\mathcal{M}^\perp} \tilde{\Theta}\|_{\text{nu}} = \sum_{i=z+1}^{\min\{d_1, d_2\}} \sigma_i(\tilde{\Theta})^q \sigma_i(\tilde{\Theta})^{1-q} \leq \rho \tau^{1-q}. \quad (\text{B.17})$$

II. We use the established $(\mathcal{M}, \overline{\mathcal{M}})$ to proceed. By decomposability (B.15) and triangle inequality, we have

$$\begin{aligned} & \|\hat{\Theta}\|_{\text{nu}} - \|\tilde{\Theta}\|_{\text{nu}} \\ &= \|\mathcal{P}_{\mathcal{M}} \tilde{\Theta} + \mathcal{P}_{\mathcal{M}^\perp} \tilde{\Theta} + \mathcal{P}_{\overline{\mathcal{M}}} \hat{\Delta} + \mathcal{P}_{\overline{\mathcal{M}}^\perp} \hat{\Delta}\|_{\text{nu}} - \|\mathcal{P}_{\mathcal{M}} \tilde{\Theta} + \mathcal{P}_{\mathcal{M}^\perp} \tilde{\Theta}\|_{\text{nu}} \\ &\geq \|\mathcal{P}_{\mathcal{M}} \tilde{\Theta}\|_{\text{nu}} + \|\mathcal{P}_{\overline{\mathcal{M}}^\perp} \hat{\Delta}\|_{\text{nu}} - \|\mathcal{P}_{\mathcal{M}^\perp} \tilde{\Theta}\|_{\text{nu}} - \|\mathcal{P}_{\overline{\mathcal{M}}} \hat{\Delta}\|_{\text{nu}} - \|\mathcal{P}_{\mathcal{M}} \tilde{\Theta}\|_{\text{nu}} - \|\mathcal{P}_{\mathcal{M}^\perp} \tilde{\Theta}\|_{\text{nu}} \\ &= \|\mathcal{P}_{\overline{\mathcal{M}}^\perp} \hat{\Delta}\|_{\text{nu}} - 2\|\mathcal{P}_{\mathcal{M}^\perp} \tilde{\Theta}\|_{\text{nu}} - \|\mathcal{P}_{\overline{\mathcal{M}}} \hat{\Delta}\|_{\text{nu}}. \end{aligned} \quad (\text{B.18})$$

By combining with the optimality in (3.4) we have $\|\mathcal{P}_{\overline{\mathcal{M}}^\perp} \hat{\Delta}\|_{\text{nu}} \leq 2\|\mathcal{P}_{\mathcal{M}^\perp} \tilde{\Theta}\|_{\text{nu}} + \|\mathcal{P}_{\overline{\mathcal{M}}} \hat{\Delta}\|_{\text{nu}}$ then we bound $\|\hat{\Delta}\|_{\text{nu}}$ by triangle inequality, (B.17), Lemma 1, $\text{rank}(\mathcal{P}_{\overline{\mathcal{M}}} \hat{\Delta}) \leq 2z$, (B.16)

$$\begin{aligned} \|\hat{\Delta}\|_{\text{nu}} &\leq \|\mathcal{P}_{\overline{\mathcal{M}}} \hat{\Delta}\|_{\text{nu}} + \|\mathcal{P}_{\overline{\mathcal{M}}^\perp} \hat{\Delta}\|_{\text{nu}} \\ &\leq 2\|\mathcal{P}_{\mathcal{M}^\perp} \tilde{\Theta}\|_{\text{nu}} + 2\|\mathcal{P}_{\overline{\mathcal{M}}} \hat{\Delta}\|_{\text{nu}} \\ &\leq 2[\rho \tau^{1-q} + \sqrt{2\rho} \tau^{-q/2} \|\hat{\Delta}\|_{\text{F}}], \end{aligned} \quad (\text{B.19})$$

which holds for any threshold $\tau > 0$. Assume $\hat{\Delta} \neq 0$, we choose

$$\tau = \left(\frac{\|\hat{\Delta}\|_{\text{F}}^2}{\rho} \right)^{\frac{1}{2-q}}$$

and then obtain (3.13).

(2) Again we use the framework established in the proof of (1). From the optimality of (3.7), we have

$$\lambda(\|\hat{\Theta}\|_{\text{nu}} - \|\tilde{\Theta}\|_{\text{nu}}) \leq \mathcal{L}_w(\tilde{\Theta}) - \mathcal{L}_w(\hat{\Theta}). \quad (\text{B.20})$$

Recall the notation in (3.10), some algebra yields

$$\mathcal{L}_w(\hat{\Theta}) - \mathcal{L}_w(\tilde{\Theta}) = \frac{1}{2} \mathcal{F}_{\mathcal{X}}(\hat{\Delta}) - \text{Re} \left\langle \frac{1}{n} \sum_{k=1}^n (\mathbf{W} \boldsymbol{\epsilon}_k) \mathbf{X}_k, \hat{\Delta} \right\rangle. \quad (\text{B.21})$$

Further use Lemma 2 and our choice of λ (3.14), we obtain

$$\mathcal{L}_w(\tilde{\Theta}) - \mathcal{L}_w(\hat{\Theta}) \leq \left\| \frac{1}{n} \sum_{k=1}^n (\mathbf{W} \boldsymbol{\epsilon}_k) \mathbf{X}_k \right\|_{\text{op}} \|\hat{\Delta}\|_{\text{nu}} \leq \frac{\lambda}{C_1} \|\hat{\Delta}\|_{\text{nu}}. \quad (\text{B.22})$$

Plug $\|\widehat{\Delta}\|_{\text{nu}} \leq \|\mathcal{P}_{\overline{\mathcal{M}}}\widehat{\Delta}\|_{\text{nu}} + \|\mathcal{P}_{\overline{\mathcal{M}}^\perp}\widehat{\Delta}\|_{\text{nu}}$ in (B.22), then combine with (B.20), and further use (B.18) which is still valid here, we obtain

$$\|\mathcal{P}_{\overline{\mathcal{M}}^\perp}\widehat{\Delta}\|_{\text{nu}} \leq \frac{C_1 + 1}{C_1 - 1} \|\mathcal{P}_{\overline{\mathcal{M}}}\widehat{\Delta}\|_{\text{nu}} + \frac{2C_1}{C_1 - 1} \|\mathcal{P}_{\mathcal{M}^\perp}\widetilde{\Theta}\|_{\text{nu}},$$

again we use triangle inequality, it yields that

$$\|\widehat{\Delta}\|_{\text{nu}} \leq \|\mathcal{P}_{\overline{\mathcal{M}}}\widehat{\Delta}\|_{\text{nu}} + \|\mathcal{P}_{\overline{\mathcal{M}}^\perp}\widehat{\Delta}\|_{\text{nu}} \leq \frac{2C_1}{C_1 - 1} \left[\|\mathcal{P}_{\overline{\mathcal{M}}}\widehat{\Delta}\|_{\text{nu}} + \|\mathcal{P}_{\mathcal{M}^\perp}\widetilde{\Theta}\|_{\text{nu}} \right] \quad (\text{B.23})$$

Then we follow (B.19) and the choice of τ in (1), (3.15) follows. \square

Proof of Theorem 1. By (3.3), (3.4) we know $\|\widehat{\Delta}\|_\infty \leq 2\alpha$. Also, recall that $\widehat{\Delta}$ satisfies (3.13). Let $\mathbf{W} = \mathbf{I}_3$. We consider the constraint set $\mathcal{C}(2, 5, \psi_3)$ where ψ_3 are slightly large such that Lemma 5 holds, i.e., there exists $\kappa \in (0, 1)$ such that with probability higher than $1 - 2(d_1 + d_2)^{-3/4}$,

$$\frac{1}{n} \sum_{k=1}^n |\langle \mathbf{X}_k, \Theta \rangle|^2 \geq \kappa \frac{\|\Theta\|_{\text{F}}^2}{d_1 d_2} - T_0 \quad (\text{B.24})$$

holds for all $\Theta \in \mathcal{C}(2, 5, \psi_3)$. By constraint in (3.4) we know

$$\frac{1}{n} \sum_{k=1}^n |\langle \mathbf{X}_k, \widehat{\Delta} \rangle|^2 = 0.$$

We rule out $2(d_1 + d_2)^{-3/4}$ probability and assume (B.24) holds. Let us obtain (3.16) by considering two possible cases.

Case 1. $\widehat{\Delta} \in \mathcal{C}(2, 5, \psi_3)$. By (B.24) we know

$$\kappa \frac{\|\widehat{\Delta}\|_{\text{F}}^2}{d_1 d_2} \leq T_0.$$

Mote that we let $\mathbf{W} = \mathbf{I}_3$, by plugging in (3.12) we obtain (3.16).

Case 2. $\widehat{\Delta} \notin \mathcal{C}(2, 5, \psi_3)$. Since we have showed that $\widehat{\Delta}$ satisfies the first, the second constraint of $\mathcal{C}(2, 5, \psi_3)$, hence it violates the third one, i.e.,

$$\frac{\|\widehat{\Delta}\|_{\text{F}}^2}{d_1 d_2} \leq \alpha^2 \sqrt{\frac{\psi_3 \log(d_1 + d_2)}{n}},$$

which also implies (3.16) under the scaling $n < d_1 d_2$ and $\rho \gtrsim (d_1 d_2)^{q/2}$. \square

Proof of Lemma 7. We let $\tilde{\epsilon}_k = \mathbf{W}\epsilon_k$, then $\tilde{\epsilon}_k \sim \mathcal{N}(0, \mathbf{W}\Sigma_c\mathbf{W})$ if viewed as 3-dimensional real random vector. To simplify the notation, we define $\tilde{\Sigma}_c$ to be $\mathbf{W}\Sigma_c\mathbf{W}$. We aim to use Lemma 4 to show the concentration property of $\|\sum_{k=1}^n \tilde{\epsilon}_k \mathbf{X}_k / n\|_{\text{op}}$, hence we first transform the rectangular matrix $\tilde{\epsilon}_k \mathbf{X}_k$ to square matrix:

$$\mathbf{S}_k = \begin{bmatrix} \mathbf{0} & \tilde{\epsilon}_k \mathbf{X}_k \\ \tilde{\epsilon}_k^* \mathbf{X}_k^T & \mathbf{0} \end{bmatrix} \in \mathbb{Q}^{(d_1+d_2) \times (d_1+d_2)}.$$

Note that $\mathbf{S}_1, \dots, \mathbf{S}_n$ are independent Hermitian random matrices with zero mean, i.e., $\mathbb{E}\mathbf{S}_k = \mathbf{0}$. Besides, it is not hard to show

$$\sum_{k=1}^n \mathbf{S}_k = \begin{bmatrix} \mathbf{0} & [\sum_{k=1}^n \tilde{\boldsymbol{\epsilon}}_k \mathbf{X}_k] \\ [\sum_{k=1}^n \tilde{\boldsymbol{\epsilon}}_k \mathbf{X}_k]^* & \mathbf{0} \end{bmatrix}$$

has the same operator norm as $\sum_{k=1}^n \tilde{\boldsymbol{\epsilon}}_k \mathbf{X}_k$, then it remains to bound the moments of $\mathbb{E}\mathbf{S}_k^l$ for $l \geq 2$. By calculation, for any $p \geq 1$, we have

$$\mathbf{S}_k^{2p} = \begin{bmatrix} |\tilde{\boldsymbol{\epsilon}}_k|^{2p} \mathbf{X}_k \mathbf{X}_k^T & \mathbf{0} \\ \mathbf{0} & |\tilde{\boldsymbol{\epsilon}}_k|^{2p} \mathbf{X}_k^T \mathbf{X}_k \end{bmatrix}.$$

We know $\mathbf{X}_k = e_{k(i)} e_{k(j)}^T$ and $(k(i), k(j)) \sim \text{unif}([d_1] \times [d_2])$, hence $\mathbf{X}_k \mathbf{X}_k^T = e_{k(i)} e_{k(i)}^T \in \mathbb{R}^{d_1 \times d_1}$, which implies that $\mathbb{E}\mathbf{X}_k \mathbf{X}_k^T = d_1^{-1} \mathbf{I}_{d_1}$. Similarly, we have $\mathbb{E}\mathbf{X}_k^T \mathbf{X}_k = d_2^{-1} \mathbf{I}_{d_2}$. Thus,

$$\|\mathbb{E}\mathbf{S}_k^{2p}\|_{\text{op}} = \frac{\mathbb{E}|\tilde{\boldsymbol{\epsilon}}_k|^{2p}}{\min\{d_1, d_2\}}.$$

Since $\tilde{\boldsymbol{\epsilon}}_k \sim \mathcal{N}(\mathbf{0}, \tilde{\boldsymbol{\Sigma}}_c)$, assume the diagonal of $\tilde{\boldsymbol{\Sigma}}_c$ is $(\tilde{\sigma}_{11}^2, \tilde{\sigma}_{22}^2, \tilde{\sigma}_{33}^2)^T$, then we know $[\tilde{\boldsymbol{\epsilon}}_k]_i \sim \mathcal{N}(0, \tilde{\sigma}_{11}^2)$, $[\tilde{\boldsymbol{\epsilon}}_k]_j \sim \mathcal{N}(0, \tilde{\sigma}_{22}^2)$, $[\tilde{\boldsymbol{\epsilon}}_k]_k \sim \mathcal{N}(0, \tilde{\sigma}_{33}^2)$

$$\begin{aligned} \mathbb{E}|\tilde{\boldsymbol{\epsilon}}_k|^{2p} &= \mathbb{E}[(\tilde{\boldsymbol{\epsilon}}_k)_i^2 + (\tilde{\boldsymbol{\epsilon}}_k)_j^2 + (\tilde{\boldsymbol{\epsilon}}_k)_k^2]^p \\ &\leq 3^{p-1} \mathbb{E}[(\tilde{\boldsymbol{\epsilon}}_k)_i^{2p} + (\tilde{\boldsymbol{\epsilon}}_k)_j^{2p} + (\tilde{\boldsymbol{\epsilon}}_k)_k^{2p}] \\ &= 3^{p-1} (2p-1)!! [\tilde{\sigma}_{11}^{2p} + \tilde{\sigma}_{22}^{2p} + \tilde{\sigma}_{33}^{2p}] \\ &\leq \frac{1}{2} (2p)!! [\sqrt{\text{Tr}(\tilde{\boldsymbol{\Sigma}}_c)}]^{2p}, \end{aligned}$$

where we use $2 \times 3^{p-1} \leq (2p)!!$ in the last line. Therefore, we obtain

$$\|\mathbb{E}\mathbf{S}_k^{2p}\|_{\text{op}} \leq \frac{1}{2} (2p)!! [\sqrt{\text{Tr}(\tilde{\boldsymbol{\Sigma}}_c)}]^{2p-2} \frac{\text{Tr}(\tilde{\boldsymbol{\Sigma}}_c)}{\min\{d_1, d_2\}},$$

showing that \mathbf{S}_k satisfies moment constraint (2.3) for even numbers under $R = \sqrt{\text{Tr}(\tilde{\boldsymbol{\Sigma}}_c)}$, $\sigma^2 = \frac{R^2}{\min\{d_1, d_2\}}$. Moreover, for $p \geq 1$ we have

$$\mathbf{S}_k^{2p+1} = \begin{bmatrix} \mathbf{0} & |\tilde{\boldsymbol{\epsilon}}_k|^{2p} \tilde{\boldsymbol{\epsilon}}_k \mathbf{X}_k \\ |\tilde{\boldsymbol{\epsilon}}_k|^{2p} \tilde{\boldsymbol{\epsilon}}_k^* \mathbf{X}_k^T & \mathbf{0} \end{bmatrix},$$

hence $\mathbb{E}\mathbf{S}_k^{2p+1} = \mathbf{0}$. By using Lemma 7, for any $t > 0$ it holds that

$$\mathbb{P}\left[\left\|\frac{1}{n} \sum_{k=1}^n \tilde{\boldsymbol{\epsilon}}_k \mathbf{X}_k\right\|_{\text{op}} \geq t\right] \leq 4(d_1 + d_2) \exp\left(-\frac{n \min\{d_1, d_2\} t^2}{2R(R + t \min\{d_1, d_2\})}\right),$$

where $R = \sqrt{\text{Tr}(\tilde{\boldsymbol{\Sigma}}_c)}$. We then plug in

$$t = 2R \sqrt{\frac{\log(d_1 + d_2)}{n \min\{d_1, d_2\}}},$$

assume $\frac{\min\{d_1, d_2\} \log(d_1 + d_2)}{n}$ is small, we have

$$\mathbb{P}\left[\left\|\frac{1}{n} \sum_{k=1}^n (\mathbf{W} \boldsymbol{\epsilon}_k) \mathbf{X}_k\right\|_{\text{op}} \geq 2 \sqrt{\frac{\text{Tr}(\mathbf{W} \boldsymbol{\Sigma} \mathbf{W}) \log(d_1 + d_2)}{n \min\{d_1, d_2\}}}\right] \leq 4(d_1 + d_2)^{-3/4}. \quad (\text{B.25})$$

Therefore, with probability higher than $1 - 4(d_1 + d_2)^{-3/4}$, (3.14) holds if we choose λ by (3.18). \square

Proof of Theorem 2. By (3.6), (3.7), we have

$$\|\widehat{\Delta}\|_{\text{w},\infty} \leq \|\widehat{\Theta}\|_{\text{w},\infty} + \|\widetilde{\Theta}\|_{\text{w},\infty} \leq 2\alpha.$$

By Lemma 7 we can rule out probability $1 - 4(d_1 + d_2)^{-3/4}$ and assume (3.14) holds, by Lemma 6 we obtain (3.15). Then we consider the constraint set

$$\mathcal{C}(2, \frac{5C_1}{C_1 - 1}, \psi_3),$$

where ψ_3 is slightly large such that Lemma 5 is valid, i.e., there exists $\kappa \in (0, 1)$ such that with probability higher than $1 - 2(d_1 + d_2)^{-3/4}$,

$$\mathcal{F}_{\mathcal{X}}(\Theta) \geq \kappa \frac{\|\Theta\|_{\text{w},\text{F}}^2}{d_1 d_2} - T_0, \quad (\text{B.26})$$

holds for all $\Theta \in \mathcal{C}(2, 5C_1/(C_1 - 1), \psi_3)$. Therefore, both (3.15) and (B.26) hold with probability at least $1 - 6(d_1 + d_2)^{-3/4}$. We show (3.19) by discussing whether $\widehat{\Delta}$ falls onto $\mathcal{C}(2, 5C_1/(C_1 - 1), \psi_3)$.

Case 1. $\widehat{\Delta} \in \mathcal{C}(2, 5C_1/(C_1 - 1), \psi_3)$, and $T_0 \leq \frac{\kappa}{2d_1 d_2} \|\widehat{\Delta}\|_{\text{w},\text{F}}^2$. Then by (B.26) we have

$$\mathcal{F}_{\mathcal{X}}(\widehat{\Delta}) \geq \frac{\kappa}{2d_1 d_2} \|\widehat{\Delta}\|_{\text{w},\text{F}}^2. \quad (\text{B.27})$$

By combining with (B.20), (B.21), (3.14), we derive an inequality

$$\begin{aligned} \lambda \|\widehat{\Delta}\|_{\text{nu}} &\geq \lambda (\|\widetilde{\Theta}\|_{\text{nu}} - \|\widehat{\Theta}\|_{\text{nu}}) \\ &\geq \mathcal{L}_{\text{w}}(\widehat{\Theta}) - \mathcal{L}_{\text{w}}(\widetilde{\Theta}) \\ &= \frac{1}{2} \mathcal{F}_{\mathcal{X}}(\widehat{\Delta}) - \text{Re} \left\langle \frac{1}{n} \sum_{k=1}^n (\mathbf{W} \boldsymbol{\epsilon}_k) \mathbf{X}_k, \widehat{\Delta} \right\rangle \\ &\geq \frac{\kappa}{4d_1 d_2} \|\widehat{\Delta}\|_{\text{w},\text{F}}^2 - \frac{\lambda}{C_1} \|\widehat{\Delta}\|_{\text{nu}} \\ &\geq \frac{\kappa \lambda_{\min}(\mathbf{W})}{4d_1 d_2} \|\widehat{\Delta}\|_{\text{F}}^2 - \frac{\lambda}{C_1} \|\widehat{\Delta}\|_{\text{nu}}. \end{aligned}$$

Further plug in (3.15), (3.18), we obtain

$$\|\widehat{\Delta}\|_{\text{F}}^2 \lesssim \frac{\rho}{(d_1 d_2)^{q/2}} \frac{d_1 d_2}{\lambda_{\min}(\mathbf{W})} \rho^{\frac{1}{2-q}} \|\widehat{\Delta}\|_{\text{F}}^{\frac{2-2q}{2-q}} \sqrt{\frac{\text{Tr}(\mathbf{W} \boldsymbol{\Sigma}_c \mathbf{W}) \log(d_1 + d_2)}{n \min\{d_1, d_2\}}},$$

by some algebra it reduces to

$$\frac{\|\widehat{\Delta}\|_{\text{F}}^2}{d_1 d_2} \lesssim \frac{\rho}{(d_1 d_2)^{q/2}} \left(\frac{\text{Tr}(\mathbf{W} \Sigma_c \mathbf{W}) \max\{d_1, d_2\} \log(d_1 + d_2)}{\lambda_{\min}(\mathbf{W})^2} \right)^{1-q/2}. \quad (\text{B.28})$$

Cases 2. $\widehat{\Delta} \in \mathcal{C}(2, 5C_1/(C_1 - 1), \psi_3)$, and $T_0 \geq \frac{\kappa}{2d_1 d_2} \|\widehat{\Delta}\|_{\text{w,F}}^2$. Then the latter inequality implies $T_0 \geq \frac{\kappa \lambda_{\min}(\mathbf{W})}{2d_1 d_2} \|\widehat{\Delta}\|_{\text{F}}^2$, we plug in T_0 (3.12), some algebra yields

$$\frac{\|\widehat{\Delta}\|_{\text{F}}^2}{d_1 d_2} \lesssim \frac{\rho}{(d_1 d_2)^{q/2}} \left(\frac{\|\mathbf{W}\|_{\infty} \alpha^2 \max\{d_1, d_2\} \log(d_1 + d_2)}{\lambda_{\min}(\mathbf{W})^3} \right)^{1-q/2}. \quad (\text{B.29})$$

Cases 3. $\widehat{\Delta} \notin \mathcal{C}(2, 5C_1/(C_1 - 1), \psi_3)$. We have showed $\widehat{\Delta}$ satisfies the first two constraints of $\mathcal{C}(2, 5C_1/(C_1 - 1), \psi_3)$, so it violates the third one, i.e.,

$$\|\widehat{\Delta}\|_{\text{w,F}}^2 \leq \alpha^2 (d_1 d_2) \sqrt{\frac{\psi_3 \log(d_1 + d_2)}{n}},$$

combine with $\|\widehat{\Delta}\|_{\text{w,F}}^2 \geq \lambda_{\min}(\mathbf{W}) \|\widehat{\Delta}\|_{\text{F}}^2$, we obtain

$$\frac{\|\widehat{\Delta}\|_{\text{F}}^2}{d_1 d_2} \leq \frac{\alpha^2}{\lambda_{\min}(\mathbf{W})} \sqrt{\frac{\psi_3 \log(d_1 + d_2)}{n}}, \quad (\text{B.30})$$

which is also dominated by the right hand side of (3.19) under the scaling $n < d_1 d_2$ and $\rho \gtrsim (d_1 d_2)^{q/2}$. So the result follows. \square

B.2 Noise Correction

Proof of Lemma 8. Let the eigenvalue decomposition of Σ_c be $\mathbf{O} \Lambda \mathbf{O}^T$, where \mathbf{O} is orthogonal matrix, $\Lambda = \text{diag}(\lambda_1, \lambda_2, \lambda_3)$ where positive numbers $\lambda_1, \lambda_2, \lambda_3$ are eigenvalues of Σ_c . We then define $\widetilde{\mathbf{W}} = \mathbf{O}^T \mathbf{W} \mathbf{O}$, which is positive definite with trace equaling 3, and we use \tilde{w}_{ij} to denote the (i,j) entry of $\widetilde{\mathbf{W}}$, so the constraint is $\tilde{w}_{11} + \tilde{w}_{22} + \tilde{w}_{33} = 3$. Then we plug in the objective, it yields that

$$\begin{aligned} \text{Tr}(\mathbf{W} \Sigma_c \mathbf{W}) &= \text{Tr}(\widetilde{\mathbf{W}} \Lambda \widetilde{\mathbf{W}}) = \text{Tr}(\widetilde{\mathbf{W}} \widetilde{\mathbf{W}}^T \Lambda) = \sum_{i=1}^3 \lambda_i \left[\sum_{j=1}^3 \tilde{w}_{ij}^2 \right] \\ &\geq \sum_{i=1}^3 \lambda_i \tilde{w}_{ii}^2 \geq \frac{9}{\lambda_1^{-1} + \lambda_2^{-1} + \lambda_3^{-1}}, \end{aligned}$$

where the first inequality is obvious, and the equal sign holds if and only if $\widetilde{\mathbf{W}}$ is diagonal, and the second inequality can be verified by KKT condition, and the equal sign is true if and only if

$$\tilde{w}_{ii} = \frac{3\lambda_i^{-1}}{\sum_{i=1}^3 \lambda_i^{-1}}, \quad \forall 1 \leq i \leq 3.$$

Therefore, the unique \mathbf{W} that minimizes $\text{Tr}(\mathbf{W} \Sigma_c \mathbf{W})$ is

$$\frac{3}{\text{Tr}(\Sigma_c^{-1})} \mathbf{O} \text{diag}(\lambda_1^{-1}, \lambda_2^{-1}, \lambda_3^{-1}) \mathbf{O}^T,$$

the result follows. \square